Master's Thesis in Environmental and Molecular Biology,

IN VIVO AND *IN VITRO* EFFECTS ON ZEBRAFISH (*Danio rerio*) AFTER NANOPLASTICS SHORT-TERM EXPOSURE.

2022-2023

Author:

Carlota Marola Fernández González

(no. 74355)

Supervisors:

Kristian Syberg, Environmental dynamics (RUC)

Ole Vang, Molecular and Medical Biology (RUC)

Louise von Gersdorff Jørgensen, Parasitology and Aquatic Pathobiology (KU)

Roskilde Universitet

KØBENHAVNS UNIVERSITET

Acknowledgements.

First and foremost, my sincere gratitude to all my supervisors, Kristian, Louise and Ole; for letting me participate in this multidisciplinary project and for giving me the opportunity of working side-by-side with you. Thank you for your guidance, support, and expertise throughout the design, performance, and analysis of this Master Thesis. I am very grateful for your continuous encouragement and your valuable lessons, my favourite: “No effect is also a good result”.

Special acknowledges to Sara, Cyril, Yajiao, Moonika and Heidi for your support, caring, and sweet treats; you were always around ready to help a colleague in need.

Thanks to Jane, Fadua and Hatice, Emil and Frederik, the booking system battles became a fun game. It has been a pleasure to share lab and worries with you.

A big shoutout to “the office of the chosen ones”, Rasmus, Naja, Kathrina, Irida, Frederik and Yahya, there was never a dull moment with you.

To Paula, my forever statistics teacher. Thanks for your patience, comprehension, and your singular way of showing me love.

Last but certainly not least to my family, Guillermo, Nuria, Medi and Pablo, it’s for you that I keep chasing my dreams. Your love has been my guiding light throughout this and all journeys.

Abstract.

Plastic contaminants and their presence in the environment is a growing concern in recent years, primarily attributed to their ubiquity and vast cumulative amounts. Approximately, 80-90% of land-based plastic pollutants are distributed through freshwater systems until they reach their final destination, the ocean. Once in the freshwater environment, the larger plastic particles, macroplastics, break down into smaller particles ending up into fragments less than 1 μm in size, referred to as nanoplastics (NPs). These NPs start accumulating in the freshwater ecosystems, posing a potential danger to the environment. This is due to its almost impossible gathering and disposal as well as the lack of understanding of its hazardous potential.

This Master's Thesis focus on Polystyrene NPs effects and accumulation by conducting two studies: (1) *in vivo* zebrafish (*Danio rerio*), focusing on embryo viability and larvae regeneration, and (2) *in vitro* embryonic fibroblast-like cell line, ZF4 (ATCC), focusing on cell viability. Both studies included experiments of short-term exposure (96 hours) to environmentally relevant NPs concentrations.

The obtained results suggest that NPs acute exposure does not have a lethal effect on embryos nor affect the natural regeneration process of the larvae. However, NPs exposure affects the larvae inflammatory process due to NPs triggering neutrophil mobilization after complete regeneration of the amputated tissue. As for ZF4 cells, NPs have been observed to be internalized into the cytoplasm, as well as a leading to a decrease in cell viability after 96 hours of exposure.

Keywords: polystyrene (PS), nanoplastics (NPs), zebrafish (*Danio rerio*), ZF4 cells, short-term exposure, ecotoxicology, cell viability.

Table of Contents

1. Introduction. 7

2. Aim of the study. 9

3. Background. 10

3.1. Plastic pollution. 10

3.1.1. Plastic definition and origin. 10

3.1.2. NPs as a hazardous particle 11

3.1.3. NPs in the environment. 12

3.1.4. NPs' presence inside cellular systems. 13

3.2. Zebrafish (*Danio rerio*) 14

3.2.1. Zebrafish as a model organism. 14

3.2.2. Zebrafish morphology and development. 15

3.2.3. Zebrafish embryo and early larvae. 16

3.2.4. Regeneration capacity. 17

3.2.5. Zebrafish NP uptake. 19

3.3. ZF4 cell line. 20

3.3.1. Cell line and cell culture. 20

3.3.2. Cell membrane and cell uptake of NPs. 20

3.3.3. Cell organelles: mitochondria and lysosomes. 21

3.3.4. Cell death vs cell apoptosis 22

4. Material and Methods 24

4.1. Zebrafish precedence and maintenance (*Danio rerio*). 24

4.2. ZF4 cell line and cell culture. 25

4.3. NP characterization. 26

4.4. Fish Embryo Acute Toxicity Test (FET, OECD no. 236). 27

4.5. Caudal fin tail amputation and regeneration. 29

4.6. Cell count assay. 30

4.7. Hoechst 33342 staining assay. 31

4.8. Confocal microscopy 33

5. Results 35

5.1. *In vivo* results 35

5.1.1. Fish Embryo Acute Toxicity Test (FET, OECD no. 236). 35

5.1.2. Caudal fin amputation and regeneration. 38

5.2. *In vitro* results 42

5.2.1. ZF4 cell culture and doubling time 42

5.2.2. Cell count and changes in morphology. 42

5.2.3. Cell viability with Hoechst 33342 staining. 47

5.2.4. Confocal microscopy 49

6. Discussion 51

***6.1. In vivo* 51**

6.1.1. Do NPs have an effect on embryos in short term exposure? 51

6.1.2. How does it affect embryo and early larvae normal development? 52

6.1.3. Do NPs have a lethal effect on embryos? 52

6.1.4. Does NP trigger an increased inflammatory response? 53

6.1.5. Does it affect normal larval processes like regeneration? 53
6.1.6. Future perspectives: *in vivo*. 54
6.2. In vitro **55**
6.2.1. Does short-term exposure to NPs have an effect on ZF4 cells? What is the effect? Is there a dose-response effect? 55
7. Conclusion. ***60***
8. References ***61***
9. Table of Figures. ***68***
10. Appendix

1. Introduction.

To this date, the world's plastic waste is distributed throughout all kinds of environments, including land-based ecosystems, freshwater ecosystems, coastal and marine ecosystems, being the last one the final destination for the vast majority of plastic pollutants (Wayman & Niemann, 2021).

It is challenging to estimate the amount of plastic generated every year, as an example, in 2015, approximately 6300 Mt of plastic waste had been manufactured, out of that, around 9% had been successfully recycled, 12% incinerated, and 79% accumulated in landfills or the natural environment (Geyer et al., 2017). Moreover, every year, almost 40% of the plastics produced are intended for single-use products -such as shopping bags, cups, or straws, being rapidly discarded. The leader in this one-time-use-only trend is plastic packaging, being present in every aspect of our daily life (da Costa et al., 2016).

On average, around 80-90% of worldwide plastic waste comes from land-based sources, most of it transported by river systems to the open sea, with a very small portion coming from ocean-based sources such as fisheries, aquaculture, commercial or private ships and coastal tourism (Cole et al., 2011; Gallo et al., 2018). Rivers play a substantial role in global plastic pollution, as they are "the arteries that carry plastic from land to sea" (The Ocean Cleanup, 2023).

In general, all kinds of freshwater ecosystems, such as rivers, lakes, streams and wetlands, are especially influenced by plastic pollution due to its proximity to the source (Redondo-Hasselerharm et al., 2020). Several studies have recently demonstrated the presence of plastic in rivers flow streams and sediments (Ballent et al., 2016; Fischer et al., 2016; Gonçalves et al., 2020); being the last ones extremely relevant because they can easily absorb and accumulate NPs as debris throughout the sediment column. These plastic particles, tend to stick and accumulate together creating hot spots areas that could endanger freshwater aquatic organisms (Redondo-Hasselerharm et al., 2020).

There is a limited number of scientific studies regarding plastic pollution in freshwater ecosystems, especially when compared to studies on marine plastic pollution. However, based on current investigations, the condition of freshwater ecosystems could be as detrimental as the pollution observed in marine environments, despite being undervalued (Azevedo-Santos et al., 2021)

It is widely known that none of the monomers used to manufacture plastic products are biodegradable, hence their prevalence in the environment (Amaral-Zettler et al., 2015; Geyer et al., 2017)Though plastic pollutants may share the same origin, they are distributed in the oceans in all kinds of forms and sizes. In function of their size, plastic fragments can be classified into: mega-, macro-, and mesoplastics (> 5 mm), microplastics (MPs, <5 mm), and nanoplastics (NPs, with a range size from 1 nm to 1 μm) (Marana et al., 2022). These micro and nanoplastics are the main components of the so-called plastic debris, being the most abundant type of litter in the aquatic environment (Redondo-Hasselerharm et al., 2020), (Iucn, n.d.). It is its small size that makes this debris untraceable and extremely difficult to remove, hence its importance and relevance as a global issue (Jambeck et al., 2015). Of all the different kinds of MPs and NPs in the environment, polystyrene is one of the most abundant (Sendra et al., 2021a).

Freshwater fishes have the highest number of documented cases of plastic ingestion, as they are also essential as a feeding source for other aquatic and terrestrial species, acting as vectors transferring and mobilising plastic materials across the trophic chain (Azevedo-Santos et al., 2021). According to several researchers, some of the direct impacts that NPs have on fishes species, and subsequently on the rest of the aquatic wildlife, include: (a) injury and death resulting from plastic entanglement to their bodies (Cole et al., 2011) (b) intestine injuries and gut distention, due to NPs attachment to the digestive tract decreasing its absorptive capacity (Cole et al., 2011) (c) gill obstruction, disabling oxygen exchange (Azevedo-Santos et al., 2021), (d) spreading of non-native pathogenic bacteria infections due to ingestion of bacteria biofilms attached on floating NPs (Rasool et al., 2021), (e) and the smothering of the seabed, creating artificial hard grounds - nanoplastic debris sinking is directly damaging the habitat of benthic organisms (Gregory, 2009). Plenty of ecotoxicology studies have already assessed toxic effects of NPs on freshwater biodiversity, from the planktonic water flea *Daphnia magna* (Kelpsiene et al., 2020), to the Brazilian amphibian *Physalaemus cuveri* (da Costa Araújo et al., 2020) and the freshwater manatee *Trichechus Inunguis* (Silva & Marmontel, 2009).

The small vertebrate zebrafish (*Danio rerio*) has earned the reputation of being a great study model for environmental risk assessment, and yet more for the determination of plastic toxicity (Bhagat et al., 2020; Silva Brito et al., 2022). Besides all the advantages that zebrafish presents as an *in vivo* model, the very presence of an already well-defined cell line (ZF4 CRL-2050™) enhances the importance of the usability of zebrafish as a model to understand overall environmental toxicity of any current or future hazard.

2. Aim of the study.

In this study, the fundamental purpose was to provide new insights into the potential short-term effects of polystyrene nanoplastic particles (PS NPs) on the vertebrate zebrafish at environmentally relevant NPs concentrations. Within this goal, two focus points were presented; 1) using zebrafish embryos and early larvae for the determination of NPs impacts *in vivo,* and 2) manipulating the zebrafish embryo fibroblast-like cell line, ZF4, for the study of cell viability after NPs exposure *in vitro.*

Two key points were highlighted for the *in vivo* study. Firstly, to identify if NPs lead to lethal or toxic effects in 0-96 hours post fertilization (hpf) zebrafish embryos; by reporting mortality, malformations, and behavioural impacts. And secondly, to determine if NPs have any impacts on natural larval processes such as the immune and regenerative response. To this aim, the regeneration rate and neutrophil mobilization after caudal fin amputation during NPs exposure were analysed.

As for the *in vitro* study, cytotoxic effects were studied by two cell viability assays, with the corresponding evaluation of live cells number after 96h of exposure to increasing concentrations of NPs. These results were coupled with live cell imaging. Additionally, three extra concerns were presented: passive entry of NPs inside the cells, accumulation of NPs within the cell and its connection with the cell's main organelles, nucleus, mitochondria, and lysosomes.

Given the results from both studies, an attempt has been made to display the correlation between cellular toxicity and animal toxicity to environmentally relevant NPs concentrations during a short-time exposure.

3. Background.

3.1. Plastic pollution.

3.1.1. Plastic definition and origin.

Plastics are synthetic, lightweight, strong, and highly durable polymers built in a very inexpensive and rapid way. In general, plastics are made of monomers extracted from oil or gas chemically bound together and biologically non-biodegradable in the environment (da Costa et al. 2016; Kwon et al. 2015). The monomers used to manufacture plastics are extracted from fossil hydrocarbons, being within the most common: ethylene for polyethene synthesis (PE), propylene for polypropylene (PP), and styrene for polystyrene (PS) (Geyer et al., 2017). Other types of plastics are polyvinyl chloride (PVC), nylon (PA), cellulose acetate (CA), and thermoplastic polyester (PET), also present in the environment at micro and nanoscales (Baig et al., 2022).

The categorization of MPs and NPs is quite new and controversial, but in the last couple of years, it has been decided to refer to NPs as those plastic particles with a diameter no larger than 100 nm in size (Ng et al., 2018). Apart from their size, both MPs and NPs can be classified as primary or secondary plastics according to their production purposes (Kanwal et al., 2023). Primary MPs and NPs are originally designed and produced in their small form for commercial use; for example, cosmetics and body care products or microfibers from clothing and other textiles, such as fishing nets. On the other hand, secondary MPs and NPs originate from the abiotic and biotic degradation of larger plastic items after environmental exposure (Mariano et al., 2021).

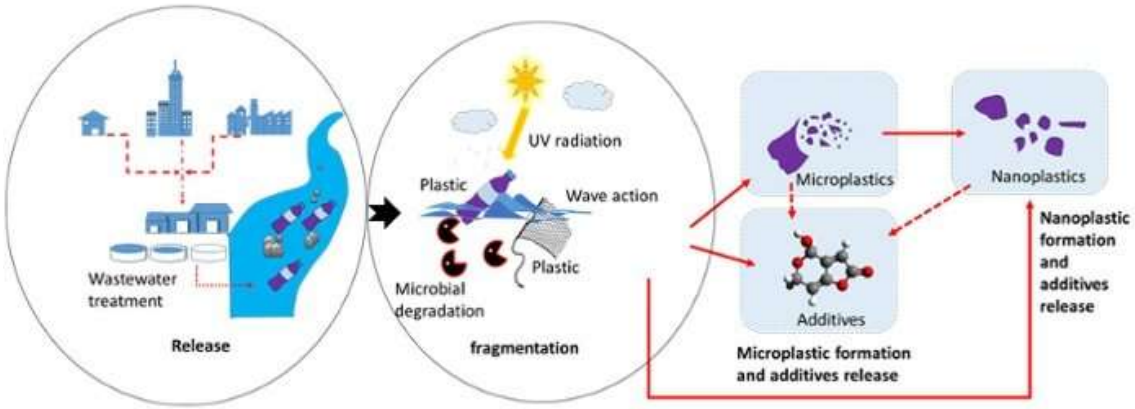

Figure 1. Plastic waste degradation in the environment. Plastic waste is released into the environment and once it gets into aquatic systems plastic degradation starts. Once in the water, plastic undergoes a fragmentation process after being exposed to UV radiation which weakens the bonds between plastic monomers, enabling other kinds of degradation such as microbial degradation and mechanical fragmentation due to wave movements. This fragmentation results in smaller plastic particles, MPs and NPs, and the consequent release of all the additives chemically attached during plastic production. (Abdolahpur Monikh et al., 2019).

As seen in Figure 1, this breakdown into smaller particles happens once discarded plastics reach the ocean environment, where photo-degradation, oxidative and hydrolytic processes driven by bacteria (Nguyen et al., 2023), weaken plastics' chemical bonds and facilitate mechanical breakdown with the water movements (Abdolahpur Monikh et al., 2019; Kwon et al., 2015).

It is stated that out of all of the MPs released into the environment, only 15-31% are primary MPs, while 70-80% are secondary MPs (Mariano et al., 2021). As for NPs, the process of gradual degradation is the predominant cause of NPs formation (Baig et al., 2022).

3.1.2. NPs as a hazardous particle

Additionally, there are several physical characteristics taken into account to categorize MPs and NPs, such as density (light enough to float or heavy enough to sink), flexibility (hard or soft), shape (fibres, fragments, pellets, granules) and the capacity to interact with other contaminants (heavy metals or organic pollutants). Depending on their intended use or purpose, plastics are often produced with certain chemical additives including pigments, lubricants, antistatic agents and flame, light and heat stabilizers (Mariano et al., 2021). In addition, among other properties present in plastic particles, due to their hydrophobicity and large surface area to volume ratio, NPs play a crucial role in the attraction of all kinds of waterborne pollutants present in aquatic environments. These chemical pollutants can easily attach to NPs, facilitating the risk of ingestion by species and their entry into the marine food web alongside NPs (Andrady, 2011). Thus, besides considering the direct toxicity of NPs, it is crucial to take into account the toxicity of the already bounded additives and the chemical pollutants that can potentially be associated with the surface of NPs (Busch et al., 2023).

Even if massive plastic production stopped completely, the problem of plastic particles in the marine environment would not go away. As mentioned above, plastics tend to break down into smaller plastic particles, but in the case of Polystyrene (PS), it is made of a type of chemical compound called styrene oligomers (SOs). When PS is manufactured, SOs are released as a by-product, in other words, another contaminant that can be leached from the weathering of discarded PS plastics into the environment (Kwon et al., 2017).

More than 100 species, ranging from zooplankton to whales, have been studied in order to understand NPs absorption through the different feeding mechanisms (Gallo et al., 2018). Aquatic species can be classified depending on their feeding strategies, such as filter-feeding where nutrients are uptaken in particles suspended in water; deposit-feeding with particles

suspended in soil; and predators that ingest all or parts of another organism, the prey. It has been confirmed that all three types facilitate NPs assimilation, by unintentional capture while feeding and by trophic transfer (bioaccumulation by the food chain) shifting NPs from the prey to the predator to facilitate the uptake of NPs, by unintentionally capturing them while feeding and by trophic transfer (bioaccumulation by the food chain) displacing NPs from prey to predator (Gallo et al., 2018). There is an alternative pathway where NPs can enter the body, through respiration, where NPs can get trapped by gill structures and easily access the bloodstream due to their small size (Bhagat et al., 2020).

3.1.3. NPs in the environment.

One of the biggest knowledge gaps concerning NPs is the real-time estimation and prediction of environmental NPs concentrations. Currently, it is really difficult to determine an accurate environmental concentration of NPs particles due to the continuous input of plastic waste and its subsequent frag(Thushari & Senevirathna, 2020)(Thushari & Senevirathna, 2020). It is estimated that not more than 2% of NPs are released during plastic production while the rest is emitted during use and after disposal phases. After disposal, NPs are either released into the environment directly or indirectly, further complicating NP tracking in the environment (Bundschuh et al., 2018). Even though there is some information about NPs production and emission coming from different countries (Figure 2), there is still an important lack of knowledge on NP quantification in the environment due to the absence of efficient and reliable analytical tools and techniques (Bundschuh et al. 2018; Pravettoni and others 2018).

One of several predictions, forecasts 1pg/l as a low hypothetical NPs concentration and 15µg/l as a high predicted environmental concentration regarding 50 nm plastic particles (Al-Sid-Cheikh et al., 2018). These concentrations are likely to increase, especially in those areas where there is some degree of plastic particle accumulation.

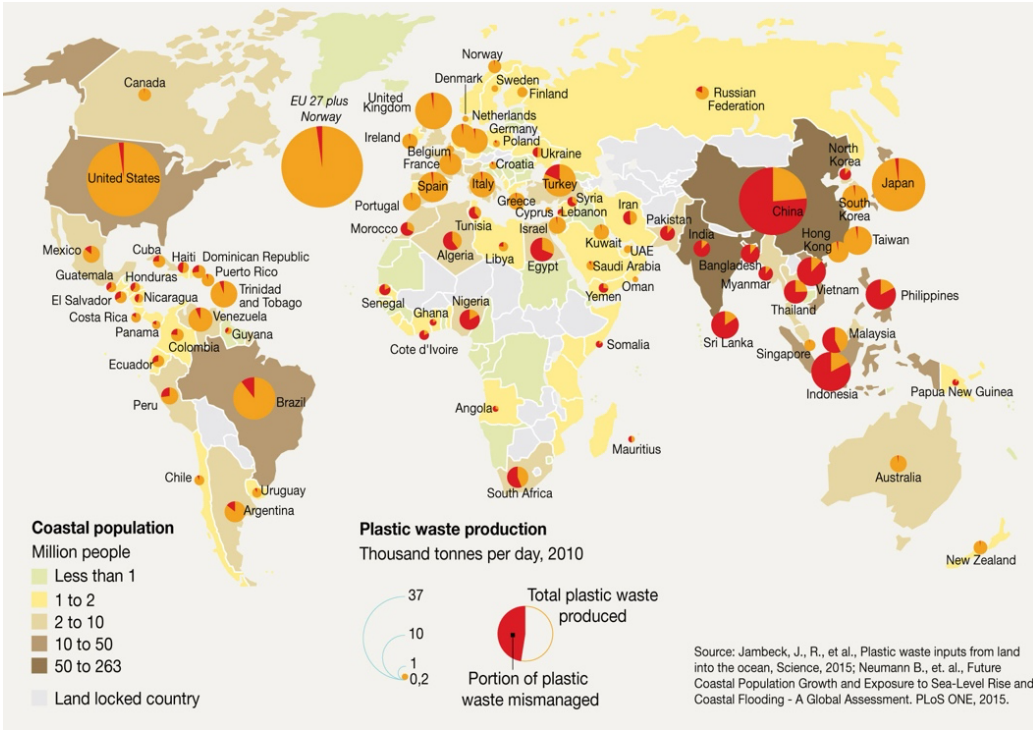

Figure 2. Plastic waste production and mismanagement around the world. It is represented how out of the total plastic production, there's a portion of plastic waste that is being mismanaged, meaning that is directly released to the environment without being recycled or re-used. (Jambeck et al., 2015)

3.1.4. NPs' presence inside cellular systems.

The uptake of NPs by living organisms and its subsequent biodistribution -transport through cells and organs, is a complex and not widely understood process (van Pomeren et al., 2017a). The two main routes of NPs input into organisms have been proven to be: direct uptake from the surrounding medium and food-based bioaccumulation. Consequently, the targeted organs for NPs' first accumulation and potential impacts are epidermis, digestive tract, and respiratory systems (Bhagat et al. 2020; Busch et al. 2023).

One of the major constraints to the uptake and transport of NPs within cells is their size (Quevedo, Lynch, and Valsami-Jones 2021; Sendra et al. 2021b). Several studies confirm the cellular uptake of NPs sized from 9 nm to 2000 nm, depending on the cell type, being macrophages and other phagosomes the most prone to uptake the biggest-sized NPs (Behzadi et al., 2017).

Also, NPs are more likely to interact with biomolecules due to their small size. NPs when in biological fluids, can be linked to proteins and lipids present in the physiological environment, developing the so-called biomolecular coronas or bio-corona. The bio-corona proteins function as a link between NPs and cellular receptors, increasing the possibility of its internalisation into the cell. (Behzadi et al. 2017; Canesi et al. 2017).

3.2. Zebrafish (*Danio rerio*)

3.2.1. Zebrafish as a model organism.

Zebrafish, also known as *Danio rerio*, is an aquatic vertebrate widely used as a model organism in biomedical research (Choi et al., 2021), behavioural genetics (Norton & Bally-Cuif, 2010) and ecotoxicology (Scholz et al., 2008). Zebrafish serve as an ideal model organism because there is great knowledge about its physiology, genetics and behaviour has been gained over the years as well as the presence of hundreds of protocols and techniques that have been optimized. Model organisms are often chosen as study models because (a) they are relevant to the specific event or matter of the study, or (b) they are outstanding on their own, without external factors or influences. They are also used because they have some key characteristics that represent a larger group of organisms beyond themselves, in this case, the rest of freshwater fishes and beyond those, vertebrates (Leonelli & Ankeny, 2013).

The implementation of zebrafish as a vertebrate model can be traced back to the 1930s, with Charles Creaser (Wayne State University, USA), however, the extensive recognition of zebrafish as a model organism is attributed to George Streisinger (University of Oregon, USA). Streisinger initially was aiming to use it for genetic studies, but he ended up optimizing care and breeding techniques, developing mutation tools, and genetic and clonal analysis among others (Meyers, 2018).

Among the features that make zebrafish a great model organism is worth highlighting: (a) its low and easy laboratory maintenance and manipulation, (b) its rapid and transparent growth and development, (c) its high fecundity rate and prolific breeding, and (d) its rich genetics (owning the same number of protein-coding genes and similar number of chromosomes as the human genome) (Meyers, 2018; Scholz et al., 2008). This study has benefited from two advantages present in the very early stages of the zebrafish: its almost complete transparency and the fast regenerative capacity of the larvae. Between the disadvantages, zebrafish require water systems with very specific parameters (pH and conductivity) that can easily fluctuate without the necessary supervision. Moreover, even though 70% of zebrafish genes have human orthologs, they own major differences such as zebrafish exhibiting a diploid genome (with the ability to duplicate) and zebrafish lacking sexual chromosomes (presenting sexual dimorphism at 3 weeks pf) (Canedo & Rocha, 2021).

Aquatic organisms are highly relevant in ecotoxicology research, yet zebrafish possess several advantages over other vertebrates also used as study models. In a recent study carried out by

Rafaella Silva in 2022, over 150 articles mentioned the use of zebrafish as a model organism for ecotoxicology purposes, where around 43% of the articles stated having worked with embryo and larvae zebrafish (Silva Brito et al., 2022). This is mostly attributed to the fact that zebrafish embryos and larvae present transparency, which makes *in vivo* imaging unchallenging. Another benefit lies in the fact that embryos and larvae take up less space and require less volume of the exposure agent for the assessment of ecotoxic pollutants.

3.2.2. Zebrafish morphology and development.

Zebrafish is a teleost fish of small body originally from South Asian freshwater ecosystems, particularly located in India, Pakistan, Nepal and Bangladesh (Meyers, 2018).

Zebrafish development is remarkably fast, with full embryonic development taking less than 72 hours at a constant temperature of 26ºC (See Figure 3). The Fish Embryo Acute Toxicity Test (FET, OECD no.236) experiment follows the embryonic and larval development from 30 minutes post-fertilization until 96 hours post-fertilization, as shown in Figure 3, where morphology and time of development are extremely important to trace irregularities during NPs exposure.

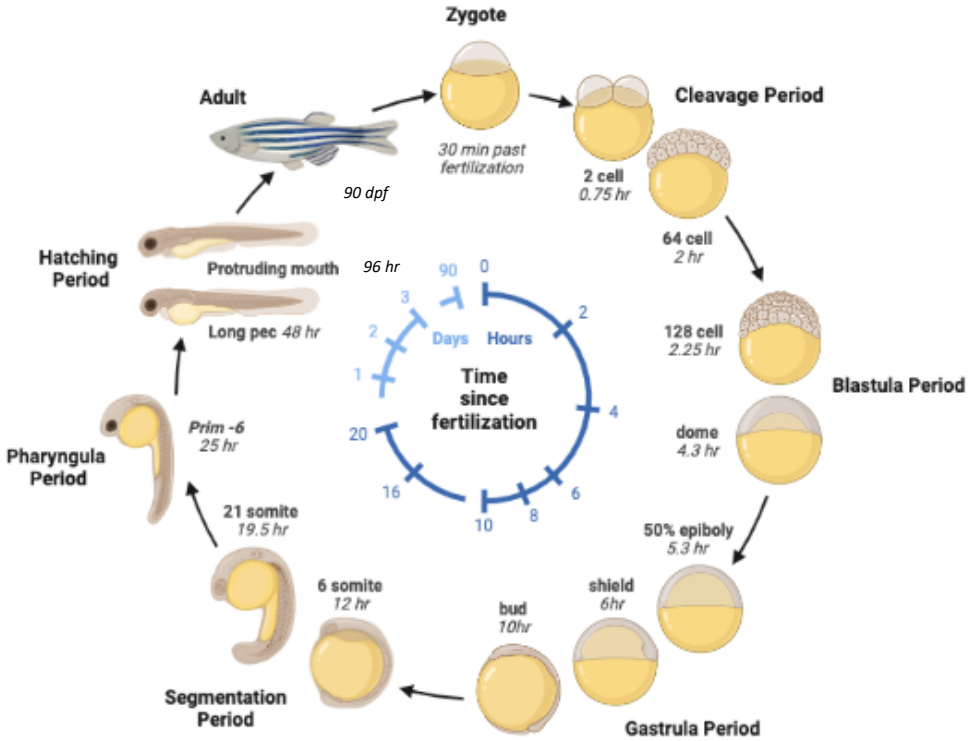

Figure 3. Zebrafish developmental timeline. From the time of fertilization until 2hpf, the zygote goes through the Cleavage period, where the cell division can be tracked from 1 single cell to approximately 200 cells. Then, the zygote enters the Blastula period, followed by the Gastrula period that will end after 10hpf with the start of the Segmentation period. In this last period, the embryo acquires a more larval-like morphology, having its peak at 48-72h with the hatching of the early larva. The next relevant process is mouth development (in protruding mouth larvae) where the yolk sac is almost all absorbed and the larva fully develops its digestive tract, the larva is ready to feed itself. From that point, the larva keeps growing and developing until 90dpf, when it becomes an adult. Made with biorrender.com.

After the embryonic period, zebrafish undergo a larval stage that lasts 4 weeks, during that time they are classified as juveniles. Zebrafish juveniles reach sexual maturity after 2.5-3 months of life, usually after reaching a size between 3-5 cm. Male and female adult zebrafish can be differentiated physically once they develop their sexual organs, for instance, females tend to enlarge their abdomen meaning that they are filled with eggs and males have a stronger yellow pigmentation on their undersides (Meyers, 2018).

3.2.3. Zebrafish embryo and early larvae.

It was necessary to understand the healthy development of zebrafish embryos in order to recognize lethality and non-lethality indicators after NPs exposure.

Zebrafish embryos, count with an eggshell consisting of two outer protein membranes, the chorion and the perivitelline membrane, that protect the embryo while acting as a barrier for contaminants, bacteria, and physical damage. The chorion contains pores of a size of 0.17 µm2 that ensures oxygen supply and at the same time avoid the intake of large compounds (Scholz et al., 2008). During the first 72hpf, the embryo's only feeding source is the yolk sac, a lipidic structure that provides the embryo with the essential nourishment before the mouth development takes place at 96-122 hpf.

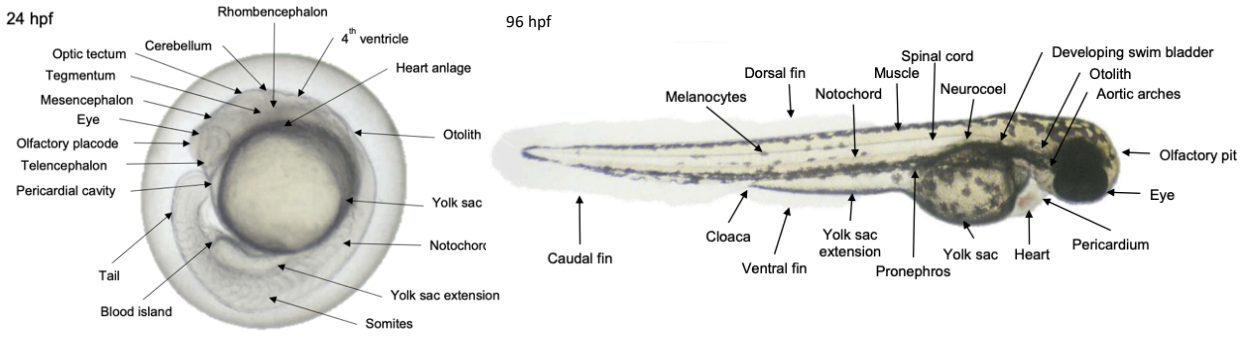

Figure 3. Morphology of a normal zebrafish embryo at 24hpf and larvae at 96hpf. Arrows indicate each structure (von Hellfeld et al., 2020).

Following the FET (OECD no.236) protocol, these are the parameters published by the Organization for Economic Co-Operation and Development (2013) as lethality indicators: (a) embryo coagulation, spotted as milky white non-transparent embryos; (b) lack of somite formation, which is defined as the absence of a segmented structure that first appears at 24 hpf, which is characterized by a spontaneous side-to-side movement called *tail curling*; (c) non-detachment of the tail bud from the yolk sac and (d) absence of heartbeat. To fully comprehend the toxicity of NPs there were some modifications to the protocol, such as the addition of more

parameters of sub-lethality. Between these, (a) motility reduction as whole-body immobilization, tail curling immobilization or pectoral fins dysfunctionality, and (b) malformations in the tail, jaw, eyes and pericardium; were recorded. Pericardium malformations are especially important because they suppose a major reduction of larvae survival (von Hellfeld et al. 2020; Wiegand et al. 2023).

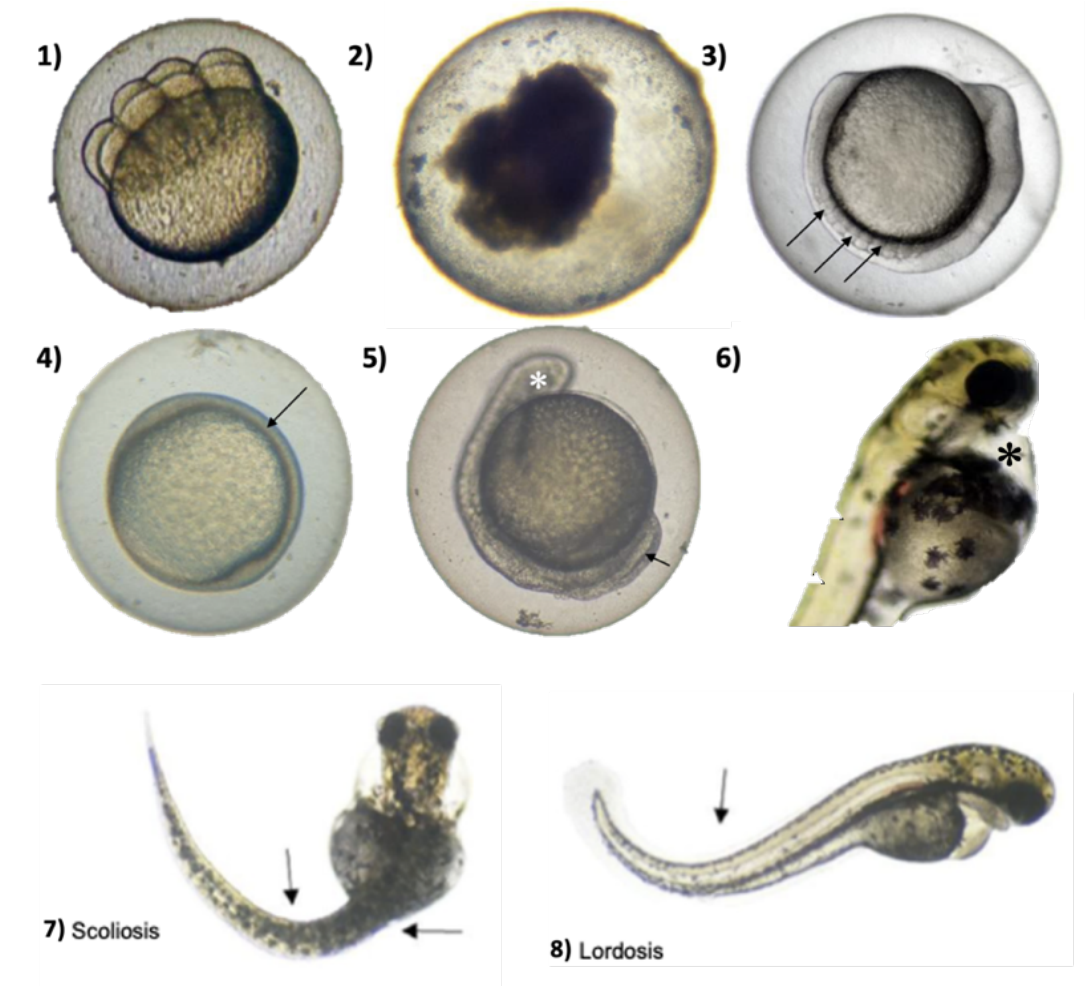

Figure 4. FET endpoints at 24h (1, 2, 3, 4, 5) and 96h (6, 7, 8). Arrows and asterisks as indicators. (1) 1.5hpf embryo at the time the exposure starts (cleavage period: 8 cells). (2) Coagulated embryo. (3) Normal somite formation (4) Lack of somite formation. (5) Non-detachment of tail bud. (6) Pericardium oedema (fluid accumulation in the heart). (7) Scoliosis (malformation). (8) Lordosis (malformation). OECD protocol and (von Hellfeld et al., 2020)

3.2.4. Regeneration capacity.

Additionally to its fast development, zebrafish larvae and adults benefit from a high regenerative capacity, being able to replace whole tissues and specialized cells, such as sensory cells (Meyers, 2018). The regeneration process consists of three main phases, starting with the epidermis covering the wound; then, the de-differentiated mesenchymal cells form a new tissue

called blastema; and finally, the appropriate tissue is formed from the blastema cells, rebuilding the original tissue morphology (Uemoto et al., 2020).

To visualize the acute inflammatory process, the use of both neutrophil and macrophages reporter lines in double transgenic larvae (DbTg (MPO, mCherry)), allows a real-time image tracking of neutrophils and macrophages recruitment during the inflammation process. Particularly during the larval stage, thanks to its optical transparency. In zebrafish embryos and larvae, immune cells are already developed at 12-16hpf in the case of macrophages and 16hpf in neutrophils, becoming functionally capable of phagocytosis by 28-30 hpf, respectively (Gray et al., 2011; Harvie & Huttenlocher, 2015). Meaning that the innate immune response to host defence is particularly early, 4-6 weeks prior to the adaptative response becomes functional (Harvie & Huttenlocher, 2015). Both leukocytes become identifiable using real-time microscopy at 48hpf (Gray et al., 2011).

The double transgenic embryos were resulting from the cross reproduction of the two transgenic lines Tg(MPX:eGFP)^{i114} (Gray et al., 2011) which owns green autofluorescence neutrophils expressing GFP protein and Tg(MpegmCherry-CAAX)$^{sh378/+}$ (Renshaw et al., 2006) whose macrophages own autofluorescence due to the expression of mCherry protein. Getting transgenic lines in zebrafish is relatively easy compared to other models due to: (a) the embryo transparency, (b) the modified zygote does not require the reimplantation in the female, (c) the fact that the zebrafish genome is duplicated allows the segmentation of 2 paralogs simultaneously, (d) the combination of genetic variants is viable (Silva Brito et al., 2022)

Neutrophils are motile phagocytic cells that own a major role in inflammatory responses since they are the first to appear in sites of injury or infection and the ones reporting inflammation resolution by triggering their apoptosis (Harvie & Huttenlocher, 2015; Renshaw et al., 2006) In zebrafish larvae, neutrophils travel from the caudal hematopoietic tissue (CHT) through the circulatory system to the site of injury, trespassing any kind of tissue. Once there, they can start phagocyting microbes, producing ROS and releasing antimicrobials, NETs (Neutrophil Extracellular Traps built by strings of DNA) and most importantly cytokines to activate and mobilize other immune cells (Harvie & Huttenlocher, 2015; Rada, 2019).

Macrophages are known for their phagocytic capacity, usually displayed during the initial phase of inflammation, and are required for limb regeneration after amputation (Nguyen-Chi et al., 2017). mCherry mutants are likely to express autofluorescence in skin xanthophores giving red fluorescence as the marked macrophages under the same UV light spectrum.

Xantophores cells are epidermal pigment cells that are developed in 48hpf larvae, presenting a major issue at the time of macrophage identification (Gray et al., 2011).

3.2.5. Zebrafish NP uptake.

Fishes present a plastic intake frequency of 72%, being oral ingestion the main route of NPs uptake and the guts the most affected organ (Sendra et al., 2021a). Even though that is a reality common in multiple marine species, regarding the Zebrafish, several studies have reported NPs accumulation in other anatomical structures such as mouth, brain, blood, liver, heart, gills, and muscles (Bhagat et al., 2020), adding respiratory and epithelial absorption to the NPs absorption routes. In contrast, NPs accumulation does not follow the same trends in embryos and larvae. During these early stages of development, zebrafish are more sensitive to NPs input and its corresponding effects. Recent studies have reported NPs accumulation in the chorion, yolk sac, endotherm, muscle fibres, eye, and spinal cord of zebrafish embryos, affecting normal growth and development and increasing inflammation and oxidative stress (Bhagat et al., 2020).

3.3.ZF4 cell line.

3.3.1. Cell line and cell culture.

The zebrafish ZF4 cell line was initially obtained from 1-day-old zebrafish *(Danio rerio)* B strain embryos by Wolfgang Driever and Zehava Rangini in 1993. During the first establishment of the cell line, only the fibroblast-like phenotype survived from among the rest of the embryo cell types (epithelial, neuronlike, melanocytes, etc) (Driever & Rangini, 1993).

ZF4 cells are differentiated cells with adherent properties growing in a monolayer structure without showing any contact inhibition signs between each other. During low cell density, the cells express a very well-defined fibroblast morphology, meanwhile, when they reach an elevated confluency they can start growing in multiple layers forming foci (points of a high concentration of cells) that eventually become round-like dead cells (Driever & Rangini, 1993).

ZF4 cells are already differentiated cells, meaning that they possess the capacity of remaining in their specialized state while undergoing continuous proliferation. Therefore, these cells are very suitable for in vitro studies offering a wide range of different applications (Baharvand et al., 2004).

Fibroblasts are eukaryotic cells present in numerous different tissues; however, the cell morphology remains frequently the same: an elongated spindle-shaped with a flattened body owning multiple cytoplasmic projections. Fibroblast's nucleus is centrally located while the rest of the organelles; mitochondria, lysosomes, a large Golgi apparatus and an abundance of rough endoplasmic reticulum, are distributed throughout the cytoplasm (Dick et al., 2023). Fibroblast morphology is significantly related to its function, to maintain and support the extracellular matrix (ECM). With their cytoplasmic extensions, they are able to interact with other cells and other components of the ECM.

3.3.2. Cell membrane and cell uptake of NPs.

The cell membrane is the main protector of the cell, shielding the intracellular components from the extracellular environment and maintaining cell homeostasis keeping ions concentrations inside of the cell. It also keeps structural support and controls the entry and exit of small molecules and nutrients (Behzadi et al., 2017).

It is known that NPs can trespass the cell membrane, although it is not done by diffusion (Barua & Mitragotri, 2014). As an alternative, NPs are internalized by endocytosis, which can be divided into phagocytosis, phagocytosis, and receptor-mediated endocytosis. It is important to

clarify that the NPs internalization mechanism depends mostly on the NP's size and the type of cells involved.

Phagocytosis is usually carried out by phagocytic cells, such as macrophages, which can surround and consume particulate matter and digest it afterwards. Non-phagocytic cells can carry pinocytosis, internalising fluids, and other molecules by forming invaginations that once the membrane closes, turn into a vesicle. Similarly, macropinocytosis involves the formation of large vesicles, internalising nonspecific cargo and large amounts of fluid (Barua & Mitragotri, 2014; Quevedo et al., 2021).

Within receptor-mediated endocytosis, there are two main types: clathrin-mediated endocytosis and caveolae or clathrin-independent endocytosis. The main difference is that the second kind operates independently of the use of the protein clathrin during the vesicle formation and that is not present in all cell types. However, they both share a similar mechanism. They fuse with the early endosomes, forming endocytic vesicles inside the cell that contain the cargo just internalised by the cell membrane. The early endosomes mature into late endosomes, which ultimately transport the uptaken material to the lysosomes, where it (Barua & Mitragotri, 2014; Quevedo et al., 2021)tri, 2014; Quevedo et al., 2021)

3.3.3. Cell organelles: mitochondria and lysosomes.

Mitochondria are a vital organelle in all kinds of cells. Between their numerous functions, production of adenosine triphosphate (ATP), generation of signalling metabolites, regulation of oxidative stress and control of apoptosis, are worth mentioning (Bakare et al., 2021).

Lysosomes are ubiquitous organelles in charge of the degradation of macromolecules either coming from material taken up from the outside of the cell or to digest components from the cell itself. Lysosomes own a variety of acid hydrolases that can only be active inside the lysosomes due to the acidic pH that is preserved inside the lysosome. This acidic pH is maintained in the lysosomes thanks to the activity of a proton-pumping V-type ATPase, which uses ATP to pump protons from the cytosol into the lysosome (Mindell, 2012).

Yang and Wang 2022, have proposed a model regarding the interaction between NPs and the cell organelles, mitochondria and lysosomes (Figure 5). Furthermore, it explains the relationship between NPs uptake and apoptosis.

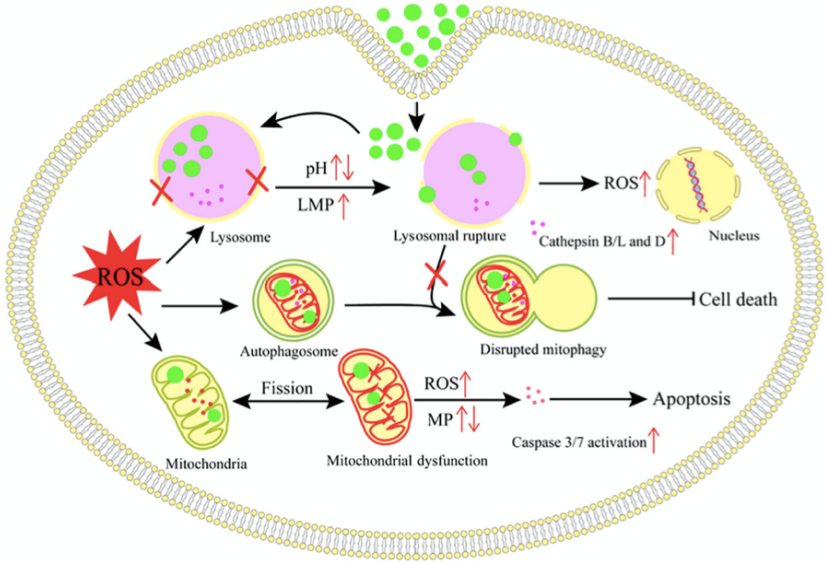

Figure 5. Mechanism of cell death after NH2-PS proposed by Meng Yang et al (2022). ZF4 cells are exposed to NPs of two sizes 100nm and 1000nm. After passing the cell membrane, NPs are deposited in lysosomes, increasing the volume of the acidic compartments (altering lysosomal alkalinization and acidification), triggering lysosomal permeabilization resulting in the release of ROS and Cathepsin B/L and D into the cytoplasm. The discharge of these molecules causes mitochondria damage and cascading effects such as caspase 3/7 activation, which provokes loss of the mitochondria cell integrity and eventually cell death. (Yang & Wang, 2022)

3.3.4. Cell death vs cell apoptosis

Cell death is a biological process resulting in an irreversible shutdown of vital cell functions and loss of cellular integrity. Apart from cell death caused by toxicants, cell death has other purposes such as: maintaining tissue homeostasis, removing unwanted or damaged cells and regulating development. There are many kinds of cell death depending on the triggering mechanisms, cell morphological alterations and the disposal of dead cells and fragments (Galluzzi et al., 2018). Three of the main types are apoptosis, necrosis, and autophagy.

Apoptosis, often referred to as programmed cell death I, is a tightly regulated and controlled process that implicates the energy-dependent activation of intracellular cascades and distinct morphological cell alterations. It occurs during normal physiological conditions, such as embryonic development and standard physiological conditions. During apoptosis, cells display various morphological changes including cytoplasmic shrinkage, chromatin condensation (pyknosis), nuclear fragmentation (karyorrhexis), and plasma membrane blebbing with the formation of whole small vesicles (apoptotic bodies) that are consumed and rapidly degraded

by phagocytic cells (macrophages, parenchymal cell or neoplastic cells), preventing the leakage of cellular contents in the surrounding tissue (Galluzzi et al., 2018).

On the contrary, necrosis is considered an uncontrolled and accidental form of cell death, where the cell follows an energy-independent death, resulting from cellular injury, inflammation, or exposure to toxins. Necrotic cells expose rapid and uncontrolled swelling (necrotic blebbing), cytoplasmic vacuoles formation, organelle damage, organelles and cell membrane rupture concluding with the release of intracellular contents into the extracellular space, which triggers inflammatory responses, attracting immune cells and potentially causing tissue damage (Barros et al., 2003; Elmore, n.d.).

Autophagy, also known as programmed cell death II, is a self-protective mechanism of cellular degradation, where cells under stress can induce this process to remove the damaged organelles and recycle their components for other cellular processes (Manshian et al., 2018). This mechanism exhibits an extensive cytoplasmic vacuolization that ends up with the consequent lysosomal degradation (Galluzzi et al., 2018).

4. Material and Methods

The totality of the *in vivo* experiments was conducted in accordance with the permit from The Animal Experiments Inspectorate under the Danish Ministry of Environment and Food (Permit: 2017-15-0201-01301).

4.1. Zebrafish precedence and maintenance (*Danio rerio*).

For the *in vivo* experiments, throughout the entire study, only freshly fertilized eggs and juvenile larvae without a protruding mouth were used. These eggs and larvae came from two zebrafish strains: Adults AB wild-type (WT) zebrafish and double transgenic (DbTg) adults Tg(MPX:eGFP)^{i114} (Gray et al., 2011) x Tg(MpegmCherry-CAAX)$^{sh378/+}$ (Renshaw et al., 2006).

All the zebrafish adults regardless of their genotype were reared in a recirculated system (AquaSchwartz, Germany) which included pH and conductivity parameters averaging 7.5 and 400 µS, respectively. The system included a light/dark cycle of 14/10 hours. This photoperiod was set to avoid algae proliferation.

Fish maintenance, as breeding conditions and egg production followed internationally accepted standards (Aleström et al., 2020). Adult care included daily feeding with two different feeding techniques: dry food ZM-300 and ZM-400 (ZM Fish Food and Equipment, UK) and alive Artemia (JBL GmbH & Co, Germany) for enhancing hunting instincts and motility. Although there was a constant circulation and renovation of water in the tanks, weekly the tanks were cleaned deeply to avoid debris (organic matter) accumulation inside of the tanks.

As for the breeding conditions, both AB wild-types and double transgenic zebrafish were handled under the same circumstances (see Figure 6). To obtain Double Transgenic eggs, pairs of males (Tg(MPX:eGFP)^{i114}) and females (Tg(MpegmCherry-CAAX)$^{sh378/+}$) were randomly chosen and placed in separated breeding tanks, resulting in 1 couple per tank. Regarding the wild-types, males and females were chosen randomly from different populations but sharing the same genotype. Also, a pair per tank. The set-up was prepared during the dark cycle so the breeding could happen as soon as the light cycle starts (8.00 am) prior to the start of the experiments. This way, the collection and sorting of the eggs could happen within the first 2 hours of development, the so-called cleavage period. During this period, it is easy to identify a healthy egg from a malformed egg or a dead egg.

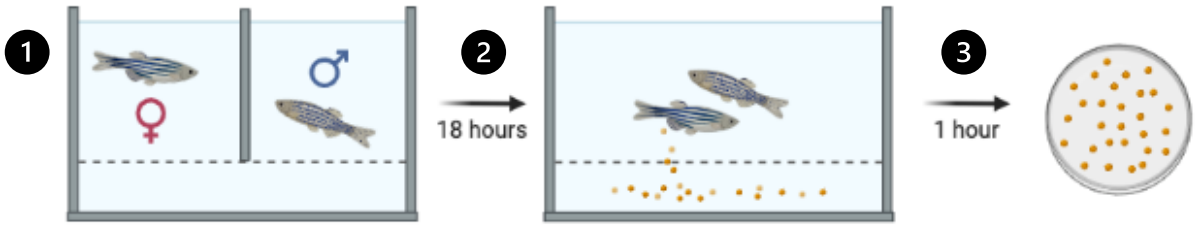

Figure 6. Breeding procedure description. (1) Sorting of females and males adults from the desired genotypes. (2) Keep in dark conditions until the start of the light cycle for the breeding process. (3) After 1 hour of mating, the eggs are fertilized and ready to be collected, counted, and sorted. Made with biorrender.com.

4.2. ZF4 cell line and cell culture.

The cell culture ZF4 CRL-2050™ (ATCC, lot: 70036276) was performed as described by the manufacturer LGC Standards GmbH (Wesel, Germany).

The cell culture was initiated from $2x10^6$ ZF4 cells in a frozen format in liquid nitrogen. These cells were thawed and seeded in a T75 flask (250 ml, 75 cm^2, Cellstar) with Dulbecco's Modified Eagle Medium, F-12 Nutrient Mixture (Gibco), supplemented with penicillin/streptomycin and 20% heat-inactivated fetal bovine serum (FBS) (Driever & Rangini, 1993; Pereira et al., 2014). For the first passages, the medium was changed every 2-3 days to ensure cell growth without disturbances. The growth conditions included a constant incubation under 28ºC and atmospheric conditions of 95% air and 5% CO2. The cell culture proceeded in T75 cm2 and T182 cm2 flasks used for cell-surface attachment.

In order to establish a ZF4 culture (Figure 7), once the cells reached a 90% confluency, regularly after 3-4 days, the cells went through a subcultivation process. In this, the old medium was removed, and cells were detached from the bottom by a short time incubation of 5 minutes with 2 ml of 0.25% Trypsin without EDTA. This was done at room temperature while checking that the cells were evenly detached from the flask surface. Consequently, to dissolve the cell aggregations, 8ml of medium containing 10% heating inactivated FBS were added to the cell suspension, and resuspended, ensuring cell disassociation. Once divided, 200 µl of the cell suspension were counted on a Coulter Counter (Beckman Coulter, Multisizer 4e). When known the cell number per ml, $2x10^6$ cells were seeded in a new T75 flask with 10ml of fresh new DMEM/F12 (with +10% FBS), making this a new passage of the cell line.

It was extremely important to make sure that the growing conditions were optimal. This cell line proved to be very sensitive to sudden changes, especially temperature and cell density.

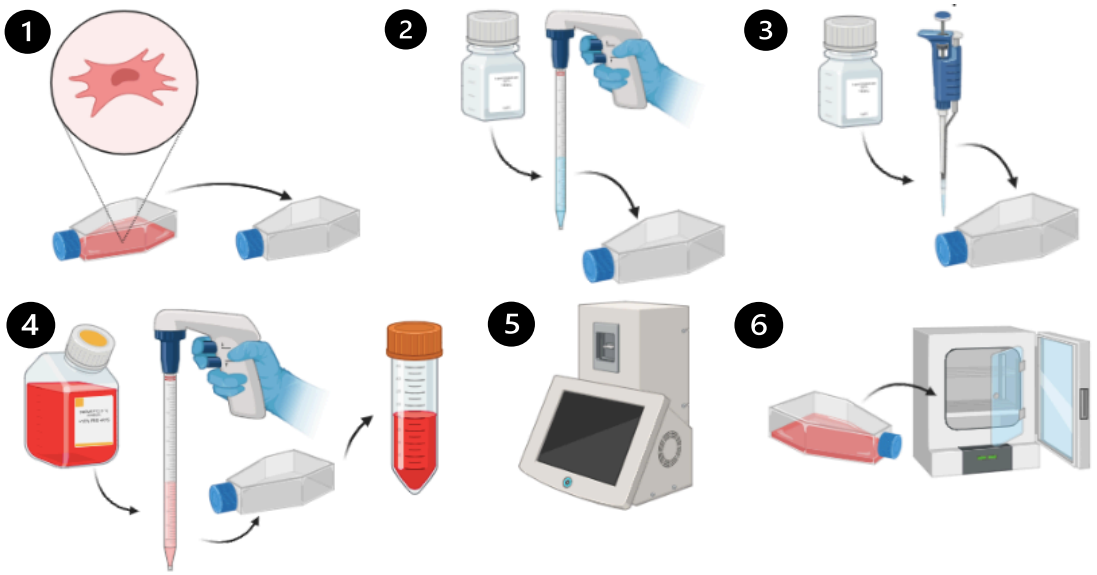

Figure 7. Subcultivation process protocol description. (1) Remove the old medium. (2) Rinse with 10 ml of Trypsin 0.25% without EDTA and remove. Add 2ml of 0.25% Trypsin without EDTA and incubate for 5 minutes at room temperature. (4) Add 8 ml of medium and resuspend breaking cell aggregations. Transfer to a 15ml Falcon Tube. (5) Use 200µl to test cell number in Coulter Counter. (6) Add 2x10^6 cells to a new T75 flask with 10ml of new medium at room temperature. Return the flask to the incubator. Made with biorrender.com.

4.3. NP characterization.

For the entire *in vivo* part, Red Fluorescent Polystyrene (PS) Latex Beads (order no. PSFR100NM) were used. These particles consisted of a diameter of 100 nm in a 2.5% concentration of solids, purchased from Magsphere Inc. (California, USA). These nanoparticles were kept in a 0.9% solvent solution of Sodium Azide. Additionally, these particles were fluorescent in UV light with an excitation/emission spectrum of 570/550 nm.

For the *in vitro* part, a new stock of nanoparticles was purchased, maintaining several characteristics with the previous ones. These were Non-Fluorescent Polystyrene (PS) Latex Beads of 100 nm (batch no. 35182), kept in a 10% solution of sterile water. The particles were purchased from Alpha Nanotech Inc. (Vancouver, Canada). Fluorescent-NPs were used in the *in vitro* exclusively for Confocal microscopy.

The NPs concentrations used for the *in vivo* experiments were set higher but included the environmentally related estimation, due to the short-time and acute nature of the experiments. The lowest concentration used was 1 mg/l while the highest was 200 mg/l (See Table 1). During the *in vitro* experiments, the concentrations were based on previous studies concerning NPs exposure to cell cultures, such as Domenech et al, 2021, where they test the cytotoxic effects of PS NPs on Caco-2 cells. Here, they aimed to simulate concentrations like what humans might be exposed to by food ingestion (i.e., 0.0011µg/ml being a potential human exposure coming from a portion of mussels) (Domenech et al., 2021). Their NPs concentration range

started from 12,3 µg/ml to 74,29 µg/ml, noticing that the highest concentration displayed a very low cytotoxic effect, meaning that the Caco-2 cell viability remained at 100% after exposure. According to this, a less broad interval of concentrations was chosen, where our lowest concentration was 0,15 µg/ml (higher than the potential concentration of a portion of mussels) and the highest was 20 µg/ml (higher than their lowest concentration since higher concentrations showed the same cytotoxic effect).

Table 1. NPs concentrations used in both in vivo *and* in vitro *studies. *Note that in the Hoechst staining method, concentrations start from 0,15µg/ml to 20 µg/ml while in the Cell Counting the lowest concentration is 1,25µg/ml. This is not followed in the in vivo part, where both sets of concentrations are strongly separated.*

***In vivo* studies (mg/ml)**	
Caudal fin amputation and regeneration	1
	10
Fish Embryo Acute Toxicity Test	12,5
	25
	50
	100
	200

***In vitro* studies (µg/ml)**	
Hoechst staining*	0,15
	0,315
	0,625
Cell Counting	1,25
	2,5
	5
	10
	20

All exposure solutions were freshly prepared immediately before their use. The stock solutions (2.5% fluorescent-NPs and 10% non-fluorescent-NPs) were kept in total darkness and at a temperature of +8ºC.

4.4. Fish Embryo Acute Toxicity Test (FET, OECD no. 236).

The potential hazard of nanoplastics on zebrafish embryos was determined following the OECD Test Guideline No. 236 (Organisation for Economic Co-operation and Development (OECD)), 2013) latest protocol. Following the test guidelines, 20 eggs per plate were exposed for a period of 96 hours under dark and static conditions. Every 24 hours mortalities and visible abnormalities related to appearance and behaviour were recorded, following the next specifications:

A. At 24h: (a) gastrulation arrest, considered as a precursor of coagulation, (b) coagulation, indicated early dead and (c) lack of somite formation or somite malformation such as somite touching the yolk sac.
B. At 48h: (a) lack of heartbeat, blood flow or blood congestion and (b) pericardium oedema (swollen pericardium full of fluid under the heart)
C. After hatching: (a) spinal malformations such as scoliosis (curvature sideways) or lordosis (strong curvature downward), and (b) motility decrease or frenetic/spasmodic movements.

The procedure started with the set-up of breeding tanks and breeding pairs of wild-type adult fish (Figure 6). Just after finishing the set-up, the dark cycle started to avoid early egg fertilization. One and a half hours before starting the experiment, the light cycle started, promoting breeding. During that time, the NP concentrations were set and the 24 well plates were filled with the desired solutions. It is important to note that every 24 well plates had 4 wells as internal control with eggs and sterile filtered water. As for the main controls, sterile filtered water was used as negative control, 4 mg/L of 3,4 dichloroaniline as positive control and sodium azide 0.9% as solvent control.

After sorting the eggs, each egg was placed in one well with 2ml of filtered sterile water and NPs depending on concentration (Figure 8). The eggs were kept in darkness and at 26ºC during the whole experiment. Images and notes were taken every 24 hours around the same time of the day as the first exposure. No physical manipulation of the eggs was carried out, just vortex of the plates every day before and after taking pictures to ensure the resuspension of nanoplastics. This test was repeated 4 times with different sets of concentrations. 12.5, 25, 50, 100 y 200 mg/L, were established as the final concentrations.

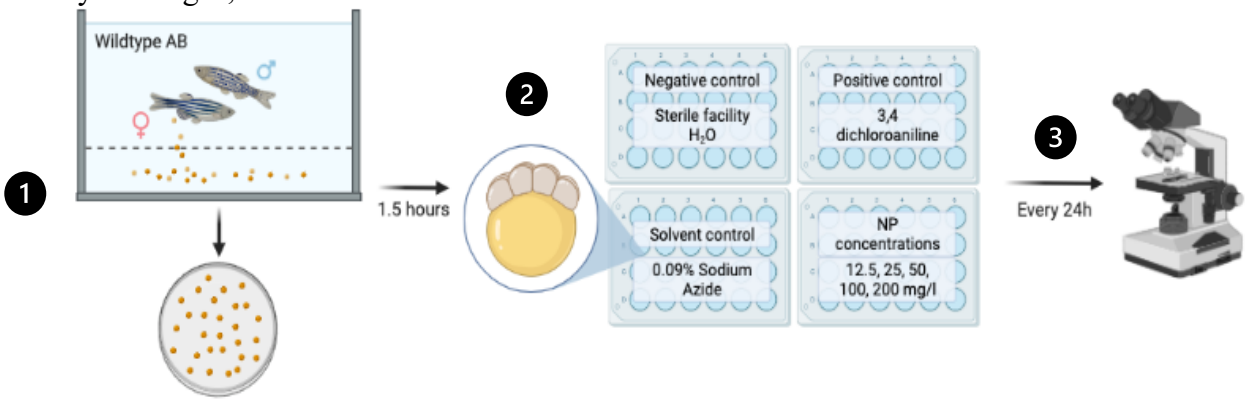

Figure 8. Fish Embryo Acute Toxicity Test protocol visualization. (1) Eggs collection and sorting 1.5 hours post fertilization following the mentioned criteria. (2) Seeding of chosen eggs in 24 wells-plates. Each plate counted with four wells as internal controls with just sterile facility water. (3) Imaging analysis every 24h to record the test parameters. Made with biorrender.com.

4.5. Caudal fin tail amputation and regeneration.

During this experiment, 3 days post-fertilization larvae were used. During those 3 days, a number of 126 WT larvae and 78 DbTg larvae were kept at 26ºC with a daily water change. Just after hatching, the now free-swimming larvae were anaesthetized with 150mg/l Tricaine Methanesulfonate (MS222, Sigma-Aldrich), leaving a number of 60 larvae as control. The study groups were divided into four categories: control no cut (without caudal fin amputation), control cut 0mg/L (larvae with caudal fin amputation that remained in sterile filtered water), cut 1 mg/L NPs (larvae with caudal fin cut exposed to 1mg/L NPs since the moment of the amputation until the end of the experiment) and 10 mg/L NPs (larvae with caudal fin cut exposed to 10 mg/L NPs since the moment of the amputation until the end of the experiment).

As shown in Figure 9, only the tip of the caudal fin was cut, ensuring that the body was not touched by the blade and that the cut was straight and clean. During the anaesthesia and the amputation, the larvae's heartbeat was recorded. Immediately after the amputation, the larvae were transferred to a Petri dish with sterile water and the subsequent NPs concentrations.

Every 24 hours after amputation, notes and images were taken from 4 larvae per sample (control, control cut, 1mg/L and 10mg/L NPs). Regenerative growth and immune cell allocation were followed for 96h, using images from a stereo fluorescence Zeiss V8 microscope (Zeiss). To take pictures, the larvae were embedded in a low melting point of 0.8% agarose gel. This gel was made of sterile filtered facility water, 1.75g/l MS222 and 0.8% of agarose (Sigma- Aldrich). Previous to the larvae handling, the gel was heated at 65ºC and kept at a constant temperature of 40ºC during the whole procedure. In the meantime, the larvae were anaesthetized in 150mg/l MS222 and transferred to a glass bottom petri dish (WillCo-dish) with a couple of drops of agarose gel. To align the larvae to the desired position a homemade tool with a 0.025mm metal thread (advent) was used. The gel was set aside for 20 minutes to solidify and then covered with a thin layer of a working solution consisting of 150 mg/l MS222 and sterile facility water to keep the larvae anaesthetized. After taking the necessary pictures the larvae were terminated with MS222.

During these months pH, conductivity and ions concentration fluctuated a lot due to a RO system change in the facility. These fluctuations didn’t affect the experiment per se but did influence the breeding process of double transgenic genotypes, decreasing the number of eggs and larvae needed to reach a statistically relevant number of samples during the whole experiment.

WT larvae were used for regeneration rate after amputation determination, while DbTg were utilized for both regeneration rate estimation and neutrophil mobilization in the regenerated tissue. Images taken from both groups were analysed with Image J2 (2.9.0/1.53 t), while the statistical analysis was performed with JASP (0.17.1 intel) and graphic representations with Graph Pad (Prism 9.5.1). Regeneration rate and neutrophil count results were analysed using the non-parametric Kruskal-Wallis test and Dunn's Post Hoc comparisons where a p-value (p) <0.005 was considered statistically significant for all calculations. An attempt to do a parametric test, ANOVA, was done. However, after following the two main assumption checks, Levene's test for equality of variances (homogeneity test) and Shapiro-Wilk for normal distribution, the assumptions were not met, therefore it was not possible to do an ANOVA.

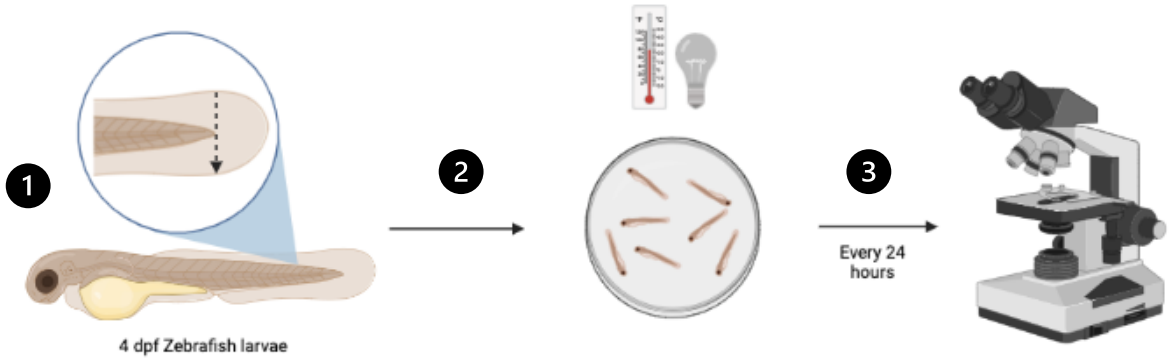

Figure 9. Fin amputation scheme. (1) Anaesthetize and fin tail cut in 4 days post-fertilization larvae. (2) Transfer of larvae to Petri dishes for recovery and start NPs exposure. (3) Imaging and analysis every 24 hours. Made with biorrender.com.

4.6. Cell count assay.

After subcultivation, the ZF4 cells were seeded in transparent 24-well plates (Greiner bio-one, Cellstar), in a number of 40.000 cells per well, accompanied by 1 ml/well of DMEM/F12. Five plates were prepared, one for time 0 hours and four for each time point: 24, 48, 72 and 96 hours. Time 0 was used to estimate the cell number 24 hours after seeding, to test the accuracy of the seeding. Consequently, after 24 hours of incubation, the cells are already attached to the bottom of the well and ready to start the exposure. After removing the old medium, Non-fluorescent NPs were added in a range of concentrations from 20 µg/ml to 1.25 µg/ml, with a dilution factor of 2. As a result, a whole plate was used for each time point, and each plate containing all 5 concentrations plus the negative control (only DMEM/F12).

Every 24h hours, as shown in Figure 10, phase contrast pictures of each well were taken using an inverted phase contrast microscope (Leica DMIRB) with magnifications at 10x and 20x. After removing the old medium of each well, 1ml of PBS without Ca and Mg was added and

rinsed twice. After that, 0.2 ml 0.25% Trypsin without EDTA was added and incubated for 20 minutes at 37°C in a humidified atmosphere containing 5% CO_2, to ensure the Trypsin activity. Once time is out, 0.8 ml Phosphate Buffered Saline without Calcium and Magnesium (HBSS) was added and steadily resuspended to ensure cell disaggregation. The cell number was estimated by Coulter Counter (Beckman Coulter, Multisizer 4e).

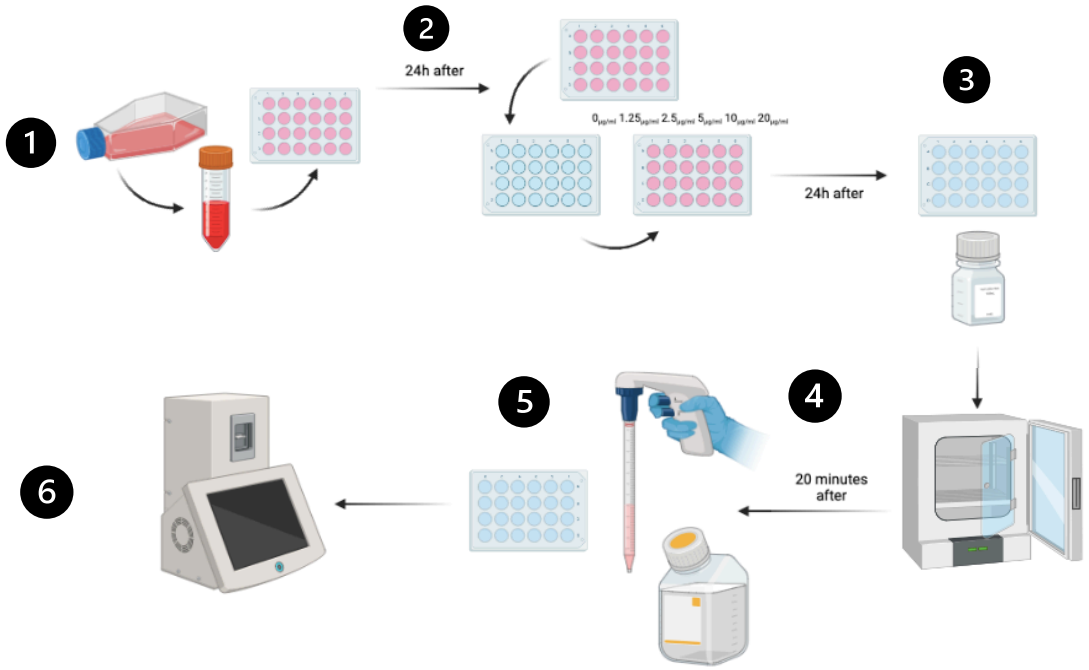

Figure 10. Cell counting assay description. (1) Subcultivation and cell number estimation. Cell seeding in 24-well plates. (2) after 24 hours, images of each well are taken. Cell exposure to NPs starts. (3) Remove the old medium. Wash the wells with 0,1 ml of PBS without Ca, and Mg and add 0,2 ml of 0.25% Trypsin without EDTA. (4) Incubate at 37º and 5% CO_2 for 20 minutes. (5) Add 0,8 ml of PBS without Ca, Mg and resuspend making enough pressure to the bottom of the wells to de-attach as many cells as possible. (6) Cell counting with Coulter Counter in 10ml of saline solution. Made with biorrender.com.

Cell imaging was processed by Image J2 (2.9.0/1.53 t), statistical analysis was performed with JASP (0.17.1 intel) and graphics and plot designs with GraphPad (Prism 9.5.1). Cell number results were analysed using the non-parametric Krustal-Wallis test and Dunn's Post Hoc comparisons where a p-value (p) <0.005 was considered statistically significant for all calculations. An attempt to do a parametric test, ANOVA, was done. However, after following the two main assumption checks, Levene's test for equality of variances (homogeneity test) and Shapiro-Wilk for normal distribution, the assumptions were not met, therefore it was not possible to do an ANOVA.

4.7. Hoechst 33342 staining assay.

The dye Hoechst 33342 (also known as bisBenzimide H 33342) is a marker dye with the capacity of binding to the double-stranded DNA grooves, retained in the nuclei of living cells.

After subcultivation, the ZF4 cells were seeded in opaque (white) 96-well dishes (Nuncleon Delta Surface, Thermo Scientific). A number of 8500 cells per well were plated with 100µl of DMEM. To avoid misleading errors columns 1 and 12 were kept free of cells, only media. After 24 hours of incubation, the old medium was removed and the cells were exposed to NPs concentrations from 20 µg/ml to 0.15 µg/ml, with a dilution factor of 2. One plate was prepared for each time point 24h, 48h, 72h and 96h.

After the suitable incubation time, as displayed in Figure 11, the cell media was replaced with DMEM F/12 medium with Hoechst 33342 dye (5 µg/mL). 100µL /well were added to each well. The wells were incubated for 90 minutes at 28°C in a humidified atmosphere containing 5% CO_2. Then, the Hoechst 33342 media was removed, and the plates were washed once with 100µL PBS with Ca and Mg added to keep the cells attached to the wells. Fluorescence intensity was measured at excitation 360 nm/emission 450 nm, with a microplate reader (Synergy HT, BIO-TEK).

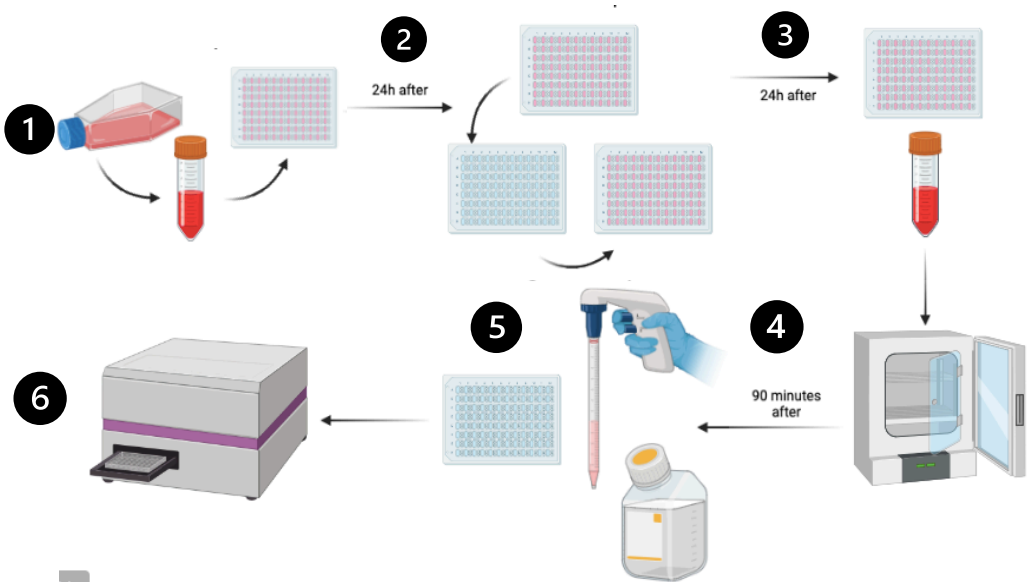

Figure 11. Hoechst staining protocol visualization. (1) Subcultivation and cell number estimation. Seeding in 96 well-plates. (2) After 24 hours, start cell exposure. (3) Remove the old medium and add 100 µl per well of Hoechst 33342 (5 µg/ml) in room temperature DMEM and incubate at 28°C and 5% CO_2 for 90 minutes. (4) 90 minutes after, remove the old medium and rinse once with PBS with Ca, Mg. Add 100 µl of PBS with Ca, Mg. (6) Read fluorescence in a microplate reader. Made with biorrender.com.

Data handling, mean calculation and inhibition figures were processed with GraphPad (Prism 9.5.1) while statistical analysis was performed with JASP (0.17.1 intel). Results were analysed using the non-parametric Krustal-Wallis test and Dunn's Post Hoc comparisons where a p-value (p) <0.005 was considered statistically significant for all calculations. An attempt to do a parametric test, ANOVA, was done. However, after following the two main assumption checks, Levene's test for equality of variances (homogeneity test) and Shapiro-

Wilk for normal distribution, the assumptions were not met, therefore it was not possible to do an ANOVA.

4.8. Confocal microscopy

Cells used for confocal microscopy needed to be cultured on poly-D-lysine-coated glass dishes for the correct attachment of the cells to the surface. The dishes (60µm-dish, 35 mm high, Ibidi) were firstly incubated for 2 hours with 400µl of 2M NaOH at room temperature. Then, the NaOH solution was removed, and the dishes were washed twice with MilliQ water. Right after, they were covered with 400µl of 500 µg/mL (H_2O) poly-D-lysine solution and incubated for 10 min at room temperature. For sterilization, the poly-D-lysine was removed, and the dishes were rinsed with 70% ethanol. Straight after, the glass dishes were ready for seeding 85.000 ZF4 cells/ml.

After four hours of incubation, the cells were exposed to 2.5 µg/ml, and 5µg/ml fluorescent NPs. A first experiment took place with the purpose of determining if the NPs could trespass the cell membrane and accumulate inside the cytoplasm. To this end, every 24h hours until reaching 72h, pictures were taken with Confocal Microscope (Olympus LSM fluoview FV 1200). The pictures were processed with Image J2 (2.9.0/1.53 t),

A second experiment was designed to perceive a more precise location of the NPs inside the cell (Figure 12). To this end, the same procedure was used but this time the cells were exposed for 48h to 5µg/ml of fluorescent-NPs (f-NPs) and 5µg/ml of non-fluorescent NPs. These were accompanied by two controls to compare mitochondria, to avoid an overlapping of red fluorescence coming from both f-NPs and the mitochondria dye (they shared the same excitation/emission state).

After 48h of NPs exposure, the cells exposed to 5 µg/ml NPs were stained with MitoTracker Orange, LysoTracker Green and Hoechst 33342. Meanwhile, the cells exposed to 5 µg/ml f-NPs were only stained with LysoTracker Green and Hoechst 33342.

For five dishes 10 ml of medium were prepared with 10 µL 400 µM Mito Tracker Yellow, 10 µL 400 µM Lyso Tracker Green and 5 µL 10 mg/ mL Hoechst 33342. Then, 2 ml per dish were added and incubated for 90 min at 28°C in a humidified atmosphere containing 5% CO_2. After the incubation time, the dishes were washed twice with 2ml each, PBS with Calcium and Magnesium. Another 2 ml of PBS w Ca/Mg were added with 10 mM glucose.

As for the confocal imaging, these were the lasers with their respective excitation/emission states used: Hoechst 33342 (350 nm /453 nm), MitoTracker Orange (554 nm / 576 nm), Lyso Tracker Green / Fitch, Laser 488 (490 nm / 516 nm) (505-521).

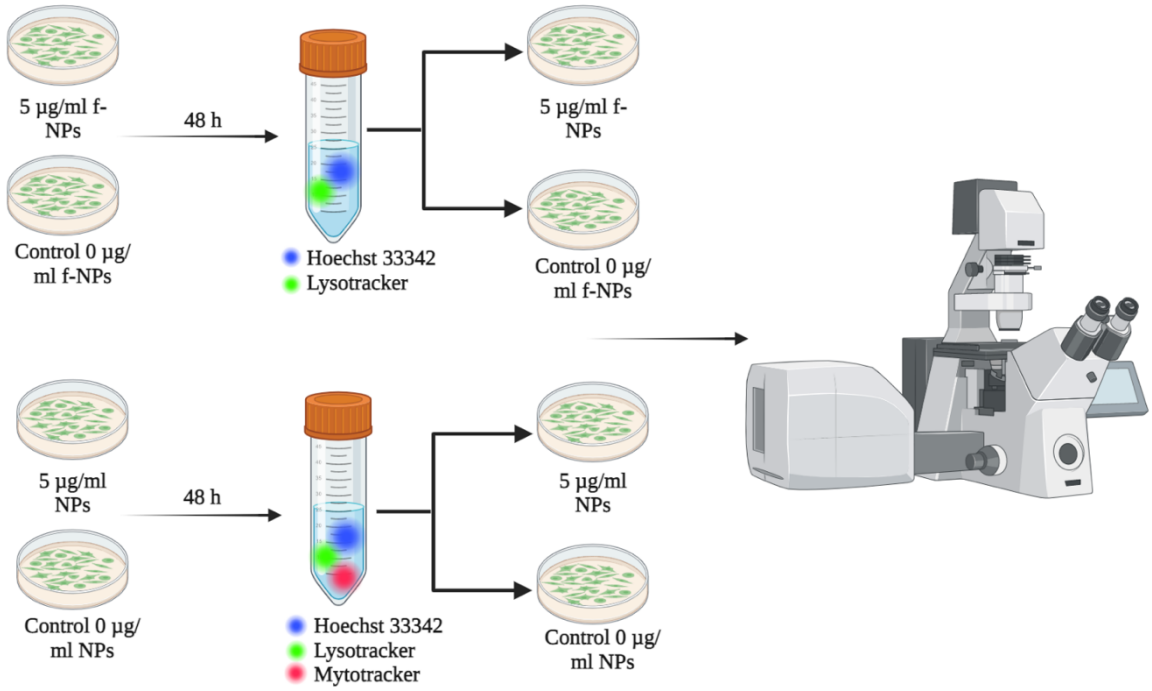

Figure 12. Visualization of the cell staining carried out for the second confocal microscopy experiment. Cells were seeded and exposed to (a) 5µg/ml fluorescent-NPS; and (b) 5µg/ml non-fluorescent-NPs on poly-D-lysine coated glass dishes. In both cases keeping a control without exposure to NPs. 48 hours after exposure, the cells were stained as represented above (a) with Hoechst 33342 and LysoTracker Green; and (b) with Hoechst 33342, LysoTracker Green and MitoTracker Orange. After waiting for the stipulated time and finishing the staining protocol, pictures were taken with the confocal microscope. Made by biorrender.com

5. Results

5.1. *In vivo* results

5.1.1. Fish Embryo Acute Toxicity Test (FET, OECD no. 236).

None of the tested concentrations reached an LC_{50} value. Four experiments with increasing concentrations were carried out until reaching 400 mg/L NP, which has not been included due to its however, none of the tested concentrations showed significant embryo mortality. To continue studying the effects of NPs in embryos following the FET protocol, sub-lethality indicators started to be recorded.

Every concentration was tested with 20 wild-type zebrafish embryos in a 24-well plate, while 4 embryos, also wild-type, were applied as internal plate control. For the whole time of the study (96 hours), both positive (3,4-dichloraniline) and negative (sterile system water) controls performed as expected, with the positive control having 85% of lethality and the negative control 0%. The solvent control (0.09% Sodium Azide) was tested non-toxic to the embryos thus it showed a 0% lethality to the exposed embryos.

At 24 hours, toxic effects were not very well-defined, and all embryos seemed to be developing normally with only one embryo presenting a swollen bud tail (Figure 14. A) found in the positive control. No coagulated embryos were found after 24 hours of exposure. At 48 hours, a heartbeat could already be recorded, facilitating mortality records, while the embryos started to move more frequently inside the eggs. At this time point, from 50 to 200 mg/L NPs the embryos showed more hectic movements than the embryos from the controls. Moreover, their eggshells presented a very high accumulation of NPs forming large aggregates coating the chorion (Figure 13, A. to E.).

At 72 hours, 70% of the embryos exposed to positive control, showed pericardium malformations (pericardium oedema, Figure 14, B. and C.) and 25% died. Meanwhile, all embryos were starting to hatch. By 96 hours all embryos had hatched, showing pericardium oedema in 70% of positive control embryos, 5% of 100 mg/l NP embryos and 15% of 200 mg/l NP embryos. Additionally, from 50 to 200 mg/l NPs the embryos displayed motility alterations (caudal fin, Figure 14, B., b.1) and pectoral fins trapped with NPs, accompanied with frenetic movements exhibited by the larvae. All internal controls showed 100% viability with 0% malformations or alterations.

Imaging results contributed further with more insights about NPs' interactions with zebrafish embryos and larvae. As shown in Figure 13, already from the lowest treatment concentration (Figure 13. A), NPs could be seen on top of the chorion but also observed inside the yolk sac, from 24 hours.

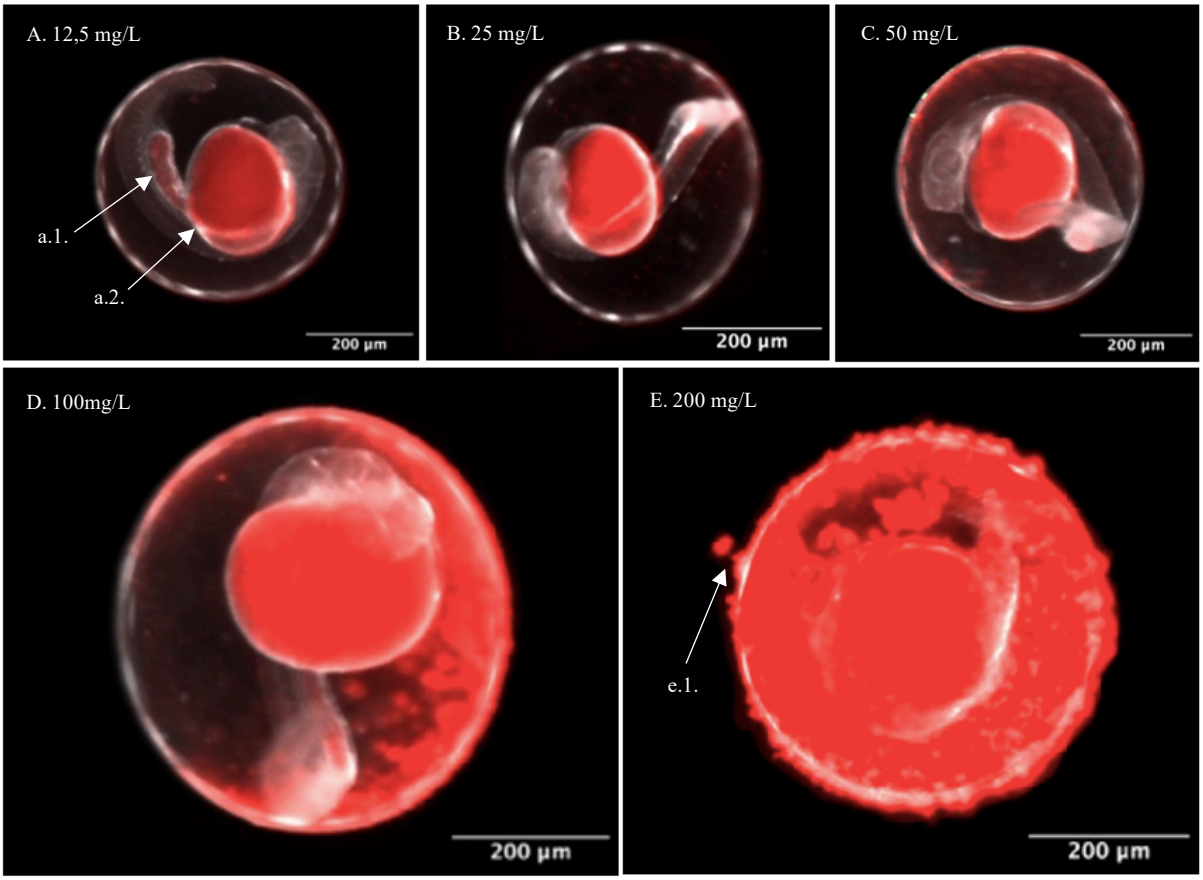

Figure 13. Zebrafish wild-type embryos after 24 hours of exposure to red fluorescent NPs. Pictures were taken under fluorescence microscopy. From A. to E. embryos exposed to increasing concentrations of NPs (mentioned above). Figure A, a.1. represents NPs accumulation inside the yolk sac extension, while a.2. points at eh NPs accumulation in the yolk sac. Figure E, e.1 indicates NPs aggregates on the surface of the chorion. Scale: 200µm.

After hatching, the accumulation of NPs aggregates on top of the chorion was still evident (Figure 14, D.). However, a substantial number of NPs was found to be accumulated inside the larvae, specifically within the olfactory pit (Figure 14. D, d.1) and the yolk sac (Figure 14. D, d.2).

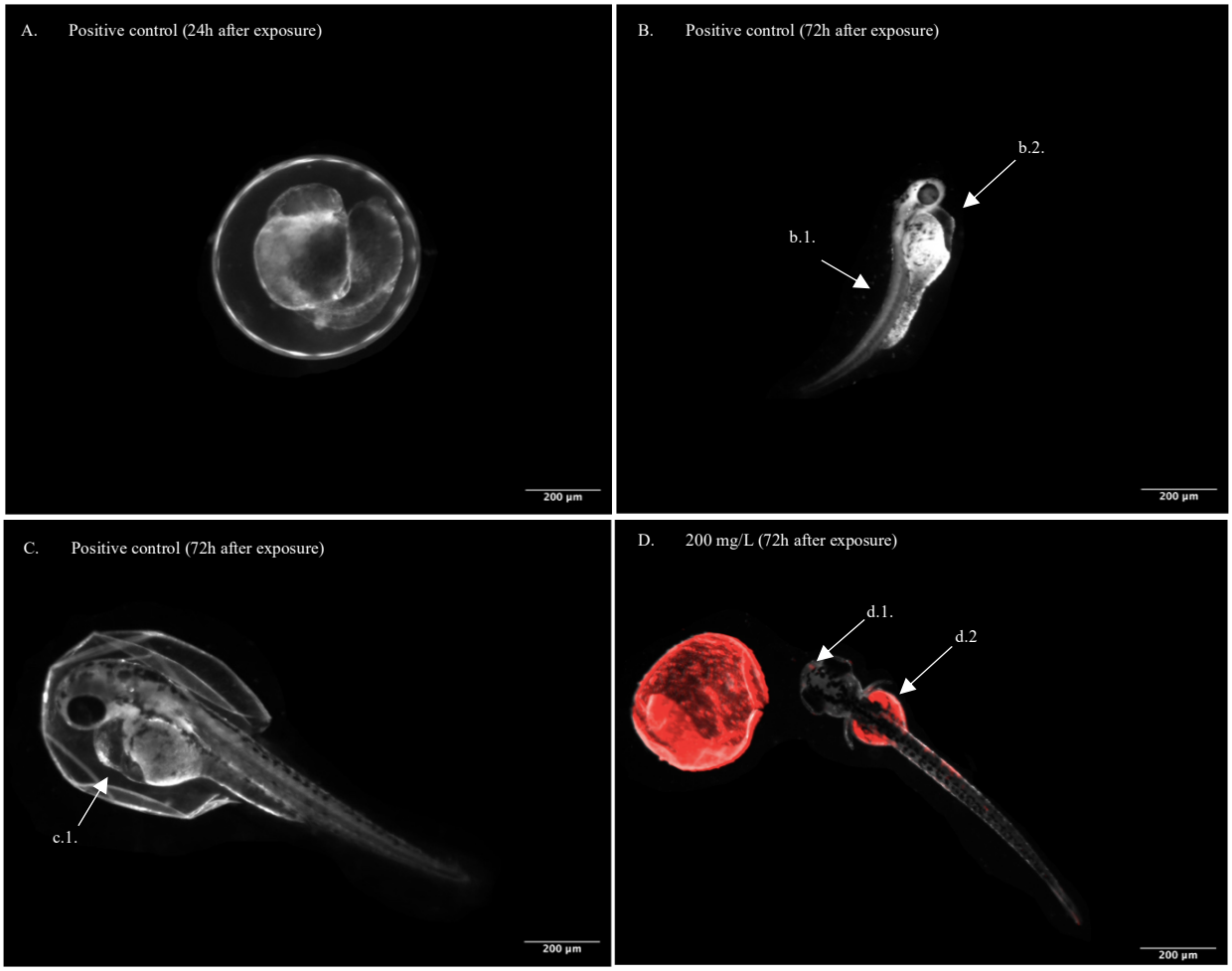

Figure 14. Zebrafish wild-type embryos and larvae under fluorescent microscopy. A. Zebrafish embryo with tail bud malformation at 24 hours after exposure to the positive control (3,4-dichloraniline). B. Zebrafish early larvae at 72 hours after exposure to the positive control (3,4-dichloraniline); b.1. indicating lordosis malformation; and b.2. implying pericardium oedema. C. Zebrafish early larvae in the moment of hatching, 72 hours after exposure to the positive control (3,4-dichloraniline); c.1. indicating pericardium oedema. D. Zebrafish early larvae 72 hours after exposure to 200 mg/L red fluorescent NPs (f-NPs); d.1. indicating f-NPs inside the olfactory pit; and d.2. indicating f-NPs accumulation inside the yolk sac and d.3. yolk sac extension. Scale: 200µm.

5.1.2. Caudal fin amputation and regeneration.

The caudal fin amputation test was performed in larvae of two lines of zebrafish; wild-types (*AB WT)* and a double transgenic larvae line with fluorescent neutrophils and macrophages (*DbTg(MPO, mCherry)).* The experiment took place for 96 hours, where pictures were taken every 24 hours and analysed by measuring the length of the regrown tail fin from the mark of amputation.

As shown in Figure 15, both groups (WT and DbTg) followed the same trends of regrowth. At 96 hours, in all concentrantions, almost the whole amputated tail was regenerated and shared a similar length as the control no cut. When comparing the regrowth trend of the treated samples against the control cut (0 mg/L), no statistical difference was shown on any of the time points. Regarding WT, the growth seemed to follow a linear continuity as the regrowth keeps increasing with time; while regarding DbTg, the regeneration rate peak was reached at 72 hours and maintained steady for the next time point.

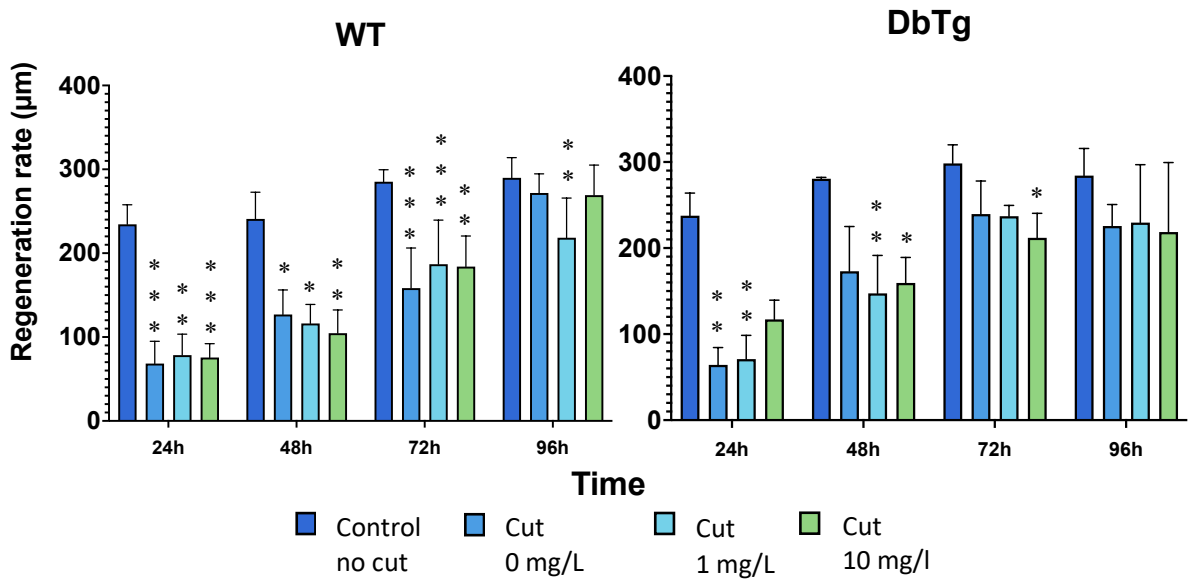

*Figure 15. Regeneration rate in wild-types (WT) and a double transgenic line with fluorescent neutrophils and macrophages (DbTg) zebrafish after caudal fin amputation. The mean of the regeneration rate in µm (±SD, n:18), is represented in the Y axis, plotted against every time point (24, 48, 72 and 96 hours), on the X axis. At the same time, the data is grouped by controls (control no cut and control cut 0 mg/l) and treatments (cut 1 mg/l and cut 10 mg/l). P-values represented the significance of the comparisons made with Duns Post Toc Test between each treatment against de control no cut. Note that: * p < .05, ** p < .01, *** p < .001.*

Simultaneously to the regeneration rate study, neutrophil mobilization in the regenerated area was followed on DbTg zebrafish. Due to macrophages sharing the same excitation/emission state and red fluorescence with xanthophores and NPs under fluorescent microscopy, macrophage mobilization could not be tracked.

In order to assess whether there was a significant distinction between the increasing concentrations of NPs and (a) the regeneration rate and (b) the number of neutrophils after amputation in the regenerated area, the non-parametric Kruskal-Wallis Test (Table 2) along with Dunn's Post Hoc Comparisons (comparisons between each concentration), were applied.

Based on the statistical analysis results presented in Table 2, the regeneration rate of double transgenic fish (DbTg) exhibited a p-value below the significance level of 0.05 for both time and NPs concentration. This provided sufficient statistical evidence to conclude that both factors significantly influence the regeneration rate in DbTg fish. Similar findings are observed in the case of wild-types (WT), where the regeneration rate was also affected by both time and NPs concentration. Furthermore, when comparing the impact of time and NPs on the regeneration rate between DbTg and WT groups, it was evident that time has a more pronounced effect than NPs. Moreover, this effect is more pronounced in WT than in DbTg.

Regarding the neutrophils, the time factor did not have a statistically significant effect on neutrophil count in the regenerated area, as indicated by the obtained p-value of 0.683. On the other hand, the NPs factor demonstratesd a significant p-value of less than 0.001, suggesting that NPs concentration significantly influences the neutrophil count.

Table 2. Kruskal-Wallis test for regeneration rate (DbTg for double transgenic and WT for wild-type) and neutrophil mobilization as variables. The factors being Time (hours) and NPs concentrations (mg/L). Statistics: statistic effect of NP concentrations on WT and DbTg regeneration rate and neutrophils number. df: degrees of freedom for each factor. p-value: the probability of the statistic to be true.

Kruskal-Wallis Test

Factor	Statistic	df	p
Time (DbTg)	30.923	3	< .001
NPs (DbTg)	20.988	3	< .001
Time (WT)	65.131	3	< .001
NPs (WT)	40.985	3	< .001
Time (Neutrophils)	1.496	3	0.683
NPs (Neutrophils)	34.800	3	< .001

After running Dunn's Post Hoc Comparison test (See Table 3) for neutrophil regeneration, during all time points, a statistical difference between the control no cut and cut 10 mg/L NPs, was shown. After 24 hours, 1 mg/L cut starts showing statistical significance when compared to the control. There is only one time point where there is a statistical difference between the control and control cut (0 mg/L), at 48 hours.

*Table 3. Dunn's Post Hoc Comparisons for neutrophil mobilization in the regenerated area between treatments. z= Dun's Post Hoc statistic that compares the variation between treatment groups. W_i and W_j= are the associated rank sums from each group of comparisons. P= statistical significance of the z-value. Note that only significant p-values are displayed. * p < .05, ** p < .01, *** p < .001*

	Comparison	z	W_i	W_j	p	
24 h	Control - 10 mg/ml	-2.520	5.625	15.167	0.012	*
48 h	Control - 0 mg/L	-2.000	3.400	11.583	0.045	*
	Control - 1 mg/ml	-3.344	3.400	17.083	< .001	***
	Control - 10 mg/ml	-2.713	3.400	14.500	0.007	**
72 h	Control - 0 mg/L	-3.112	3.800	15.500	0.002	**
	Control - 10 mg/ml	-2.906	3.800	14.100	0.004	**
96 h	Control - 1 mg/ml	-2.332	2.833	11.400	0.020	*
	Control - 10 mg/ml	-2.522	2.833	12.100	0.012	*

As displayed in Figure 16, at 96 hours it seems that there is a big difference in neutrophils number between the control cut (0 mg/L) and the exposed cuts (1 and 10 mg/L). During the first time points, control cut 0 mg/L shows a growing in number tendency up to 72 hours. At 96 hours there is a drastic drop in neutrophils number. For cut 1 mg/L, during the first hours, there is no such difference in neutrophil number, but at 96 hours neutrophil number reaches its peak point, almost 11 neutrophils on average in the regenerated area. Meanwhile, cut 10 mg/L follows the same trend as cut 0 mg/L with a continuous increase of neutrophils number even at 96 hours.

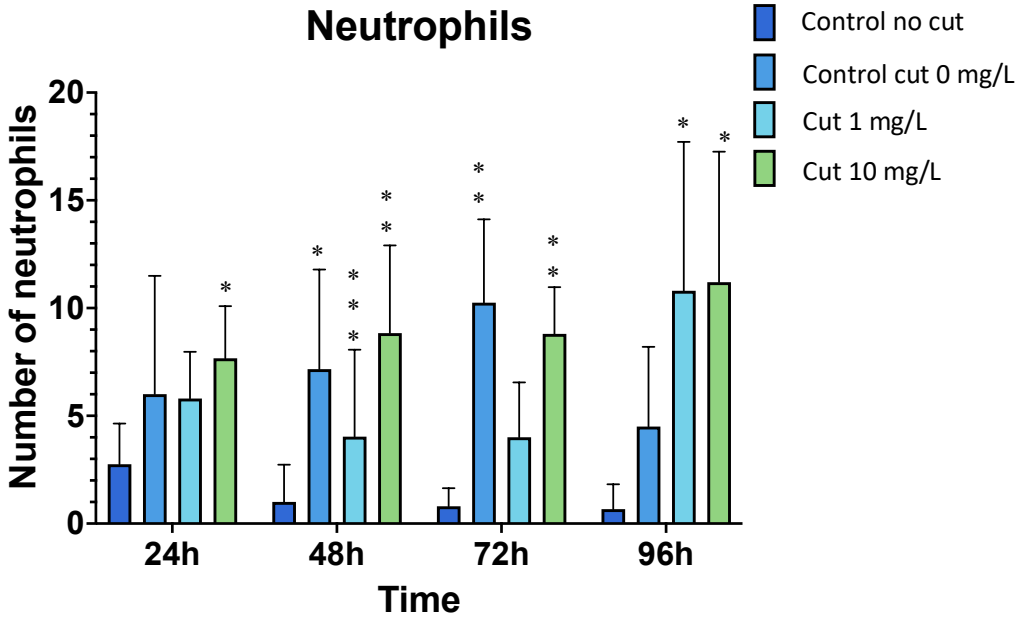

*Figure 16. Bar plot of neutrophils number in regenerated area of Double Transgenic (DbTg) zebrafish after caudal fin amputation. The dependent variable, the number of neutrophils (±SD, n:6), is represented in the Y axis, plotted against every time point (24, 48, 72 and 96 hours), in the X axis while being grouped by controls (control and control cut 0 mg/L) and treatments (cut 1 mg/L and cut 10 mg/L). P-values represented the significance of the comparisons made with Duns Post Toc Test between each treatment against de control no cut. Note that: * p < .05, ** p < .01, *** p < .001.*

All these data points were coupled with fluorescence microscopy as shown in Figure 17. In cut 10 mg/L, throughout all the time points, red fluorescence can be seen as a background composed of red fluorescent NPs, macrophages and xanthophores.

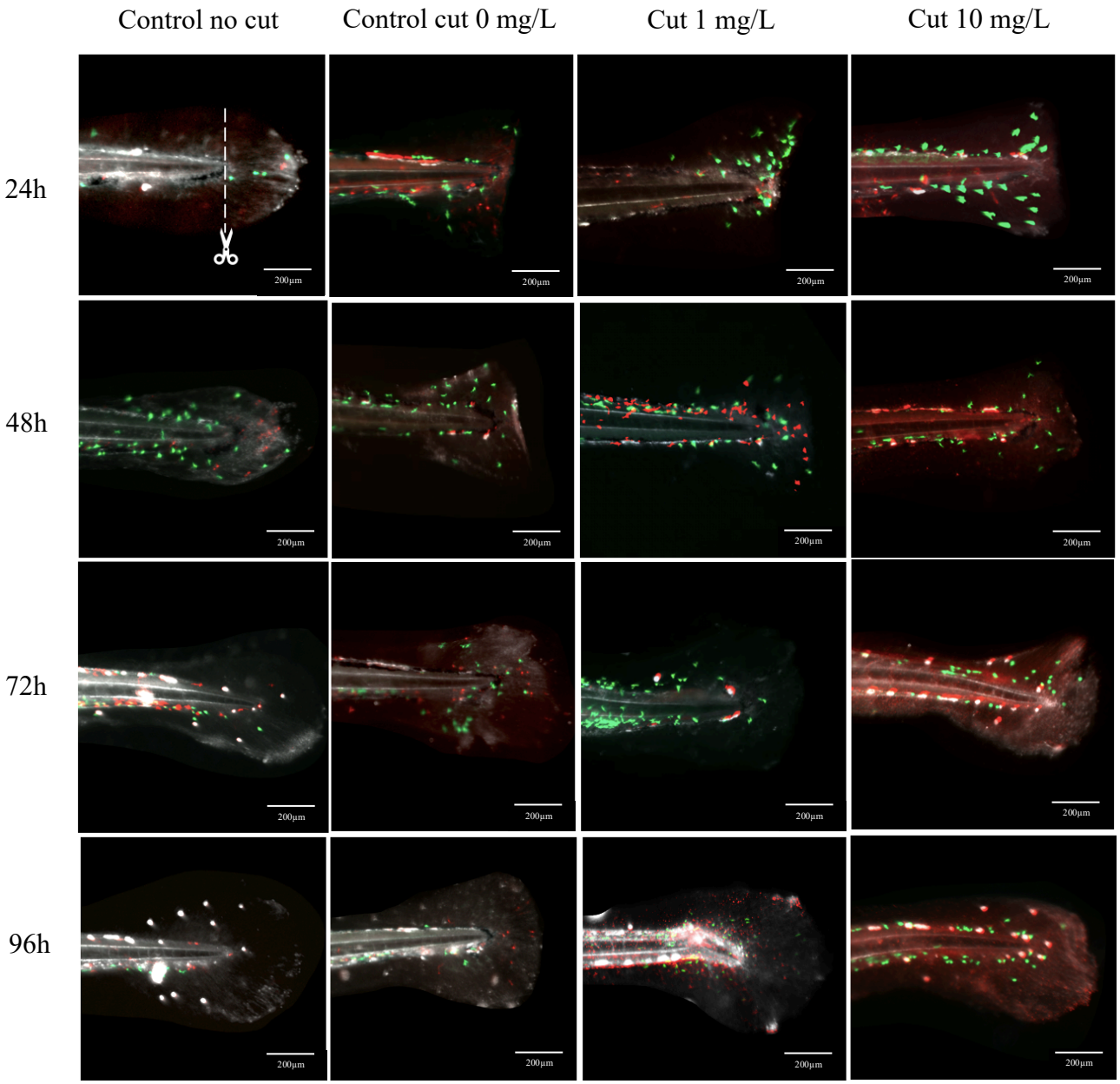

Figure 17. Caudal fin amputation and regeneration through the different time points. Neutrophils are represented in green. Macrophages, xanthophores and NPs in red. Note in Control 24 hours it is indicated where the cut was performed. The cut was made through the whole tail fin, being careful to not touch the body of the zebrafish larvae. Scale: 200µm.

5.2. *In vitro* results

5.2.1. ZF4 cell culture and doubling time

After purchasing the ZF4 cell line, the challenge of producing a worthy and consistent culture of ZF4 cells was acquired. There was null experience with the handling of this cell line and very limited literature about its subcultivation, so every protocol had to be optimized in order to succeed in generating a large ZF4 culture for the current and future investigations.

The term cell doubling time refers to the amount of time a cell takes to double itself, giving rise to two cells, hence doubling the population.

After the first 3 months of cell culture, cell doubling time started with an estimated value of 1.5 weeks (P1). After changes in the cell medium (DMEM/F12) by adding +20% of inactivated fetal bovine serum (FBS) and permitting the cell culture to reach a high confluency, around 80% confluency, the cell doubling time could be assessed.

The ZF4 cell doubling characterization was done under the subcultivation process in a total of three 24-well plates, where every plate corresponded to one time point (24, 48 and 72 hours). Only cells grown in DMEM/F12 +20% inactivated FBS, were used for the experiment.

Table 4. Cell doubling time (T, in hours) comparison of ZF4 cell number and their corresponding time combinations. Every 24 hours for 72 hours, a new result was added to the table where it was compared against each other. Note that: t1 equals time 1 while, t2 equals time 2. At the same time, Q1 refers to the mean of the total cell number from 24 replicates at t1, and Q2 to the mean of the total cell number from 4 replicates at t2.

$T(h) = (t2 - t1) \times \{\log(2)/[\log(Q2/Q1)]\}$

Doubling time (h):	115,65	71,37	57,79	46,23	41,87
t1(h)	0	0	0	24	48
t2 (h)	24	48	72	72	72
Q1 (ZF4 cells)	50.000	50000	50000	57735	79695
Q2 (ZF4 cells)	57735	79695	118576	118576	118576

These results (Table 4) showed that the higher the population number, the lower the cell doubling time.

5.2.2. Cell count and changes in morphology.

The cell count assay was performed to determine ZF4 cell viability by tracking the number of living cells after NPs exposure. Additionally, changes in cellular morphology were followed with phase contrast microscopy.

As mentioned in the Material and Methods section, for the set-up of this experiment, 40.000 cells per well were intended to be seeded. However, the results at time 0 (time of the exposure) showed a decrease in the seeding success of almost 65%, with an estimated cell number of 14.000 cells seeded per well. This number was the cell number of reference for tracking the cell growth over time in both control and NPs concentrations.

After the data collection, a graphical representation (Figure 18) of the mean of the number of cells was made, plotting the cell number against each time point. At 24 hours there was not a significant difference between treatments, but the highest concentration (20µg/ml). At both 48 and 96 hours, a trend following the dose-response effect could be appreciated, meaning that the cell number appeared to be decreased with increasing NPs concentration over time. At 48 hours after exposure, the control (0 µg/ml NPs) exhibited a cell number of 22.613 cells, while the highest concentration (20µg/ml) showed a cell count of 10.464 cells, meaning that the cell number decreased by almost 50% after exposure. The same trend was followed with the rest of NPs concentrations during this time point.

After 72 hours, almost all the results from the treatments fell into the same range of cell number, without any statistically significant difference against the control and increasing NPs concentrations. It could also be seen that this time point owned the highest data variability, represented by the error lines (±SD). There was no clear dose response or any sign of trend.

The dose-response effect was revealed again at 96 hours, where the control (0µg/ml) cell number increased its size up to 29.412 cells, while at 20 µg/ml, the cell number shows a value of 7.486 cells. In other words, under 20µg/ml NPs concentration, ZF4 cells showed a decrease of 75% in cell growth against the control. The trend was followed at all NPs concentrations.

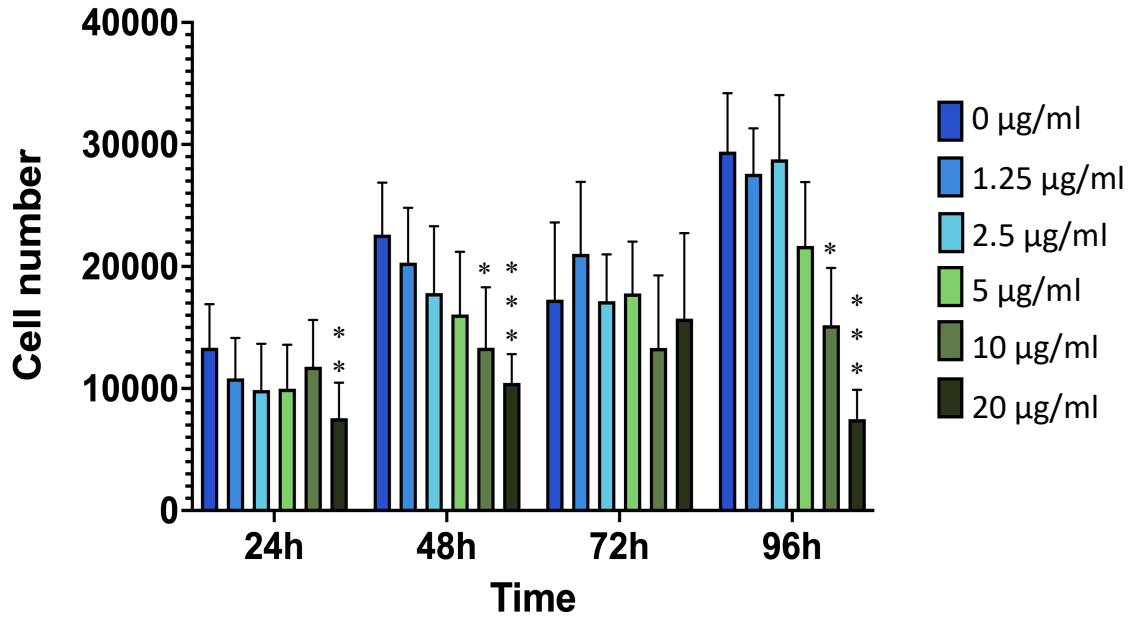

*Figure 18. Effect of NPs on ZF4 cell number. The dependent variable, mean of the cell number of 3 replicates (±SD, n:12), is represented on the Y axis, plotted against every time point (24, 48, 72 and 96 hours); on the X axis, while remaining grouped by increasing NP concentrations. Each time point represents a different 24-well plate, meaning that for "48 hours" the 24-well plate was not disturbed until the exposure time was reached. Each colour represents the different NP concentrations, cells were exposed to. P-values represented the significance of the comparisons made with Duns Post Toc Test between each NP concentration against de control. Note that: * p < .05, ** p < .01, *** p < .001.*

Simultaneously to the execution of cell counting assay, phase-contrast microscopy pictures were captured in order to keep track of morphological changes in the exposed cells. After 24 hours of exposure (Figure 19), a gradual loss of cytoplasmic projections could be appreciated, leading into a more round-like cell morphology (Figure 19, F.).

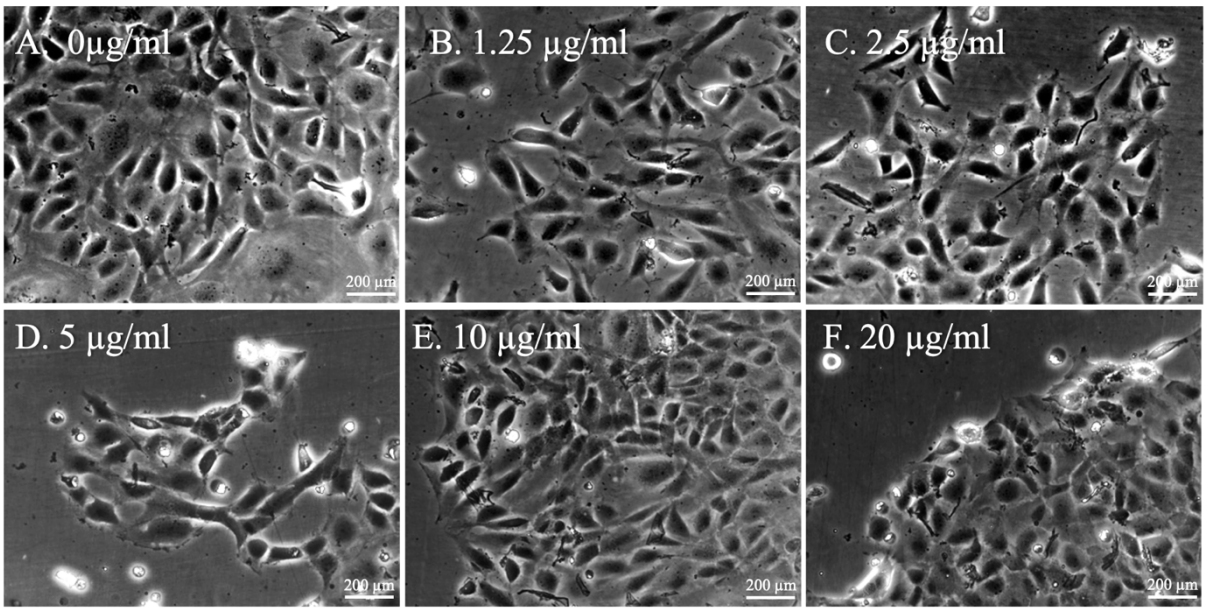

Figure 19. ZF4 cells after 24 hours of NPs exposure. Each picture, from A to F, corresponds to the cells exposed to each NPs concentration (from 0 to 20 µg/ml). Scale: 200 µm.

Furthermore, at 48 hours (Figure 20), a large confluency (95%) at the control and at 1.23 µg/ml (Figure 20, A. and B.) could be observed. At 2.5 µg/ml (Figure 20, C.) a lesser cell growth was seen, matching the low confluency of the cells. At higher concentrations, from 5 to 20 µg/ml (Figure 20, D., E. and F.), clear signs of cell death started to be detected. These structures owned a round-like morphology and seemed to be completely empty inside, only keeping a perfect membrane layer attached to what looks like the remains of dead cells. These dead cells appeared floating in the medium, however, at 10µg/ml (Figure 20, E., e.1), the same cell structure was still attached to the surface with some cells already detaching from the rest.

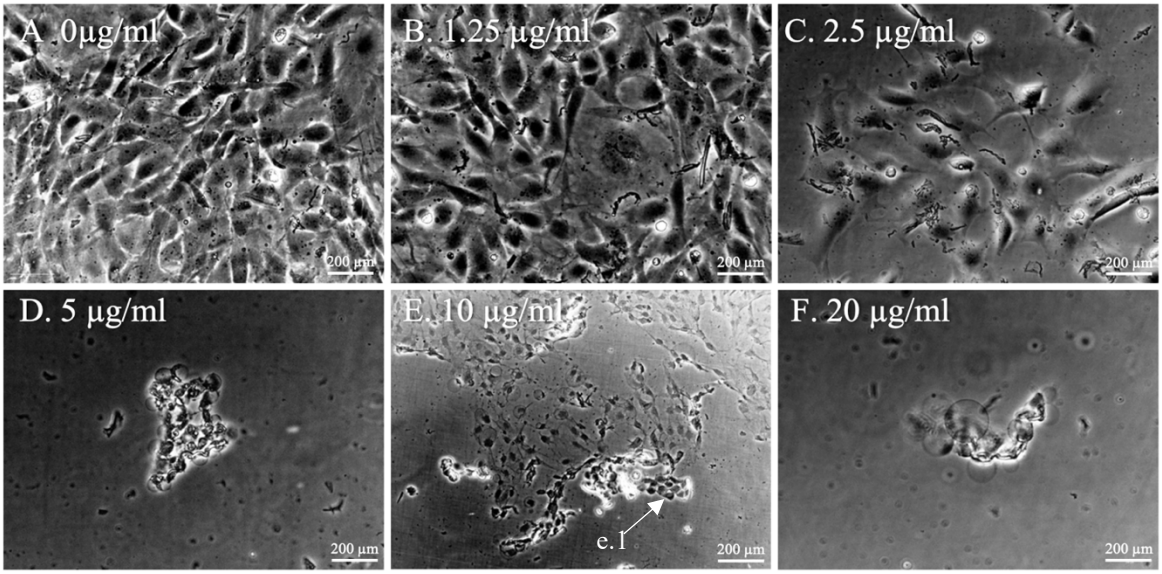

Figure 20. ZF4 cells after 48 hours of NPs exposure. Each picture, from A to F, corresponds to the cells exposed to each NPs concentration (from 0 to 20 µg/ml). Scale: 200 µm.

At 72 hours, the imaging results were not concluding, showing cell death though all the concentrations (Figure 21).

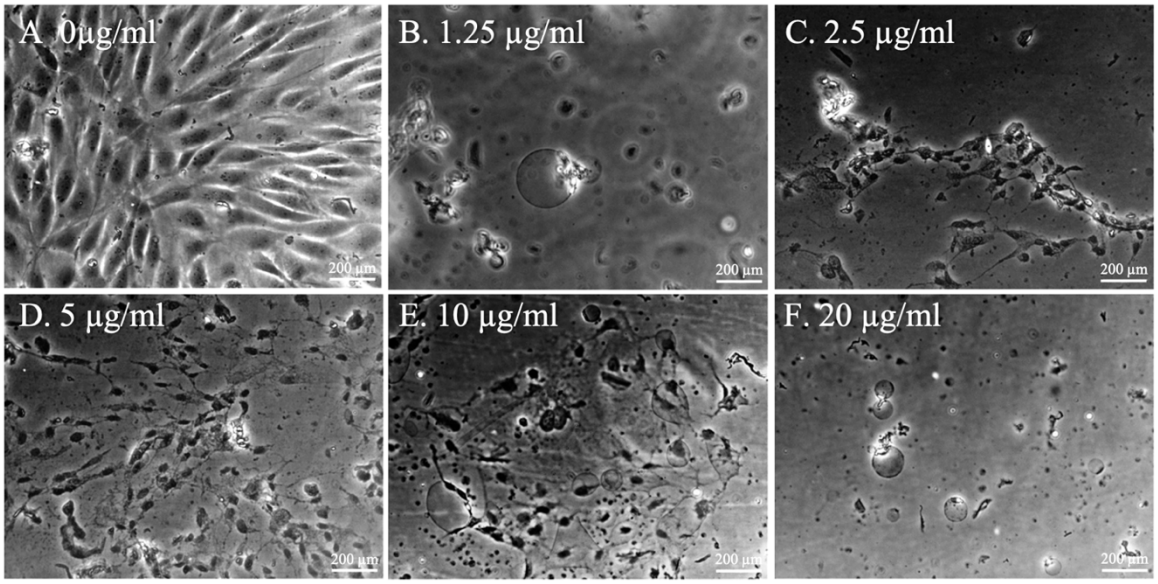

Figure 21. ZF4 cells after 72 hours of NPs exposure. Each picture, from A to F, corresponds to the cells exposed to each NPs concentration (from 0 to 20 µg/ml). Scale: 200 µm.

At 96 hours (Figure 22), a new kind of dead cells could be appreciated starting from (Figure 22, A.) 0µg/ml, and increasing in number during the following concentrations, 1.25 µg/ml and 2.5 µg/ml (Figure 22, B. and C.). These dead cells owned a round-like shape and under phase-microscopy they could be spotted white and bright. However, in the higher concentrations, from 5 to 20 µg/ml (Figure 22, D., E. and F.), the previously described dead cells were seen again. The cells shared the same characteristics and they appeared both attached to the surface or floating in the medium.

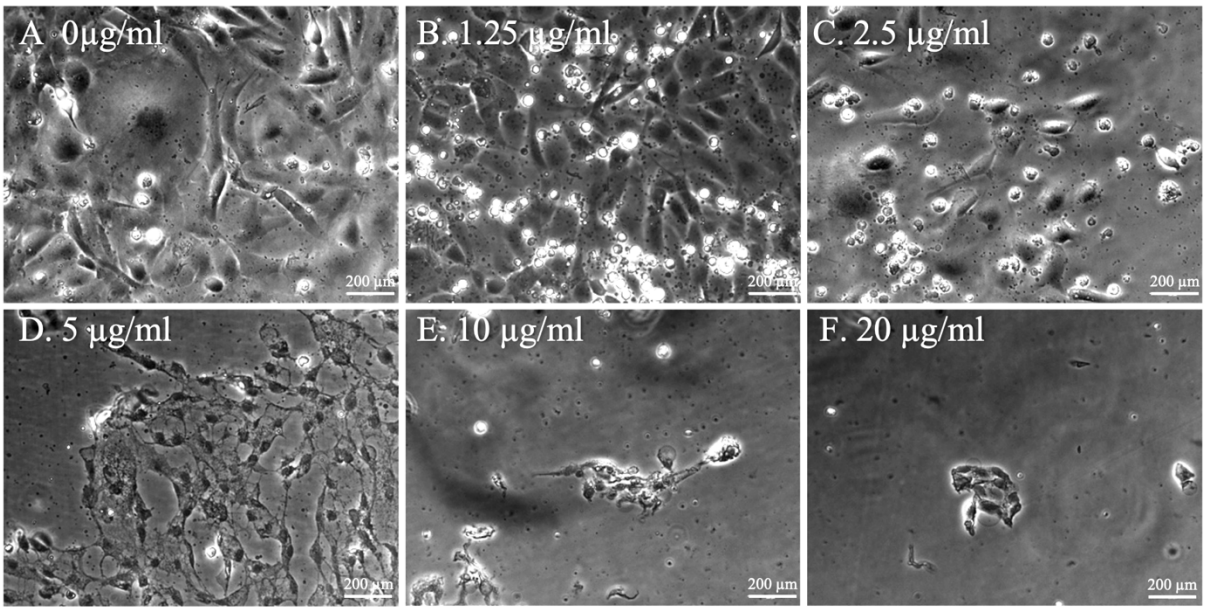

Figure 22. ZF4 cells after 96 hours of NPs exposure. Each picture, from A to F, corresponds to the cells exposed to each NPs concentration (from 0 to 20 µg/ml). Scale: 200 µm.

To evaluate whether there was a statistically significant difference between the increasing concentrations of NP and the number of living cells, the non-parametric Kruskal-Wallis Test (Table 5) with the corresponding Dunn's Post Hoc Comparisons (comparisons between each concentration, (Table 6) were applied. As seen in Table 1, the p-value obtained was <.001. With a value below 0.05 of significance level, the null hypothesis was rejected, meaning that the NPs concentration have a statistically significant effect on cell number reduction. Both factors seem to have a similar effect on the cell number, considering that the difference between both statistic values is minimal.

Table 5. Results from the Krustal-Wallis test to determine if there is an effect on cell number by different factors: Time (hours) and NPs concentrations (µg/ml). Statistic: statistic effect of NP concentrations over ZF4 cell number. df: degrees of freedom for each factor. p-value: probability of the statistic to be true.

Factor	Statistic	df	p
Time (h)	28.107	3	< .001
NPs Concentrations (µg/ml)	28.058	5	< .001

As shown in Table 6, there was a highly significant p value within all the comparisons against the highest concentration (20 µg/ml), the highest effect being observed in the comparison between 0 and 20µg/ml (z= 4.341). There was no significant difference between the smallest concentrations (0-5 µg/ml).

*Table 6. Dunn's Post Hoc Comparisons regarding NP-concentrations and cell number, through 96 hours of exposure. Note that * p< .05, ** p < .01, *** p< .001. z= Dun's Post Hoc statistic that compares the variation between treatment groups. W_i and W_j= are the associated rank sums from each group of comparisons. P= statistical significance of the z-value.*

Comparison	**z**	**W_i**	**W_j**	**p**	
0 - 10	2.843	64.563	36.563	0.004	**
0 - 20	4.341	64.563	21.813	< .001	***
1.25 - 10	2.589	62.063	36.563	0.010	**
1.25 - 20	4.087	62.063	21.813	< .001	***
2.5 - 10	2.018	36.563	56.438	0.044	*
2.5 - 20	3.516	56.438	21.813	< .001	***
5 - 20	2.818	21.813	49.563	0.005	**

5.2.3. Cell viability with Hoechst 33342 staining.

Continuing with an alternative assay for cell number determination, Hoechst 33342 staining was performed on ZF4 cells to determine the % of cell inhibition after exposure to NPs. Under this procedure, cell number after exposure was obtained by measuring the emitted fluorescence from the Hoechst dye attached to the DNA of the living cells. The results were considered reliable when the negative control (0 µg/ml, DMEM) presented a mean value of 0% inhibition effect on ZF4 cells.

As shown in Figure 23, the XY line graph showed the relationship between NP cell inhibition % and each NP concentration. The plot suggested an overall low dose-response inhibition effect, without reaching 25% inhibition. The highest inhibition impact was observed during the first 24 hours, with its peak point being +21.41 inhibition % at 20 µg/ml NP.

It was also shown how the lowest NP concentrations (0.15 and 0.315 µg/ml) at the first three time points, had a higher inhibition effect than when doubling the NP concentration (0.625 µg/ml). At 0.625 µg/ml instead of amplifying the inhibition effect, it decreased independently of the three first time points; for instance, -2.702 at 24 hours and -5.468 at 72 hours. Unpredictably, at 24 and 72 hours the general trend was the same with different inhibition rates: at 0.625 the inhibition % decreases for both time points followed by an increase of inhibition % up until 5 ug/ml, it falls again at 10 µg/ml and rises again at 20. However, this trend was not

followed at 96h, where the highest inhibition % laid at 0.625 µg/ml, while in general a more linear tendency was displayed.

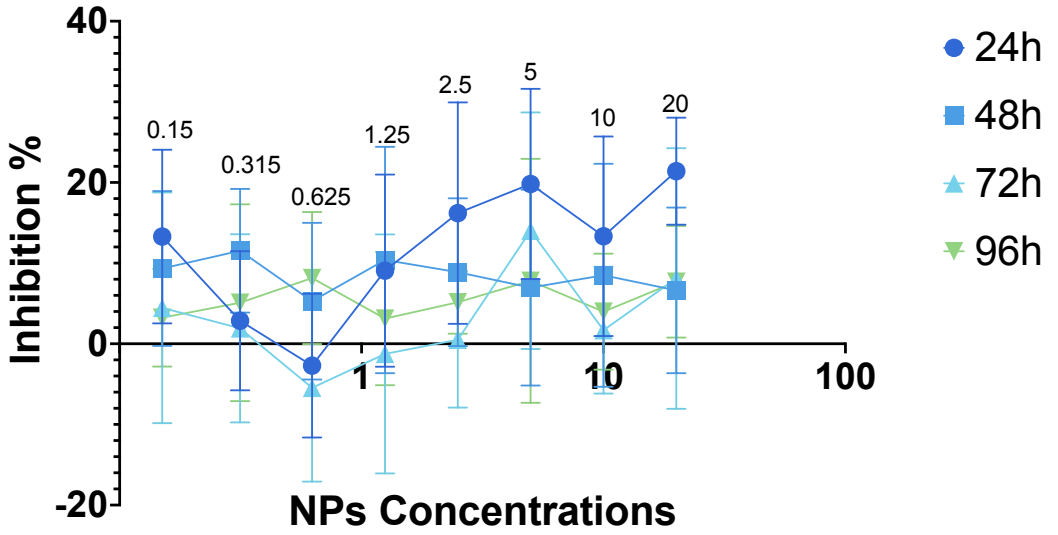

Figure 23. Inhibition % of NP on ZF4 cells under increasing concentrations: 0.15, 0.315, 0.625, 1.25, 2.5, 5, 10, 20 µg/ml NP (shown on top of error lines). Note that the concentrations are plotted on their log10 form. Control (0µg/ml) is not represented but it equals 0% inhibition. Each line joins together the different points which represents the mean of the NP inhibition % (± SD, n=24) on cells exposed to the previously mentioned concentrations. The four sets 24, 48, 72 and 96 hours represents the exposure time.

As seen in the graphic representation, the clearest low-response effect is shown at 24 hours, therefore, this time period was chosen as a cut off period to assess whether the concentrations have a statistically significant difference between the increasing concentrations of NP and the number of living cells. A non- parametric Kruskal-Wallis test was used, thus, as seen in Table 7, the p-value obtained was <0.01, therefore, the null hypothesis was rejected, in other words, there is enough statistic evidence to say that there was an effect of NP concentrations on cell viability at 24 hours.

Table 7. Results obtained from Krustal-Wallis Test to assess whether the NPs concentration influences ZF4 cells inhibition % after 24h of exposure. Statistic: statistic effect of NP concentrations over ZF4 cell inhibition %. df: degrees of freedom for each factor. p-value: probability of the statistic to be true.

Factor	Statistic	df	p-value
Concentration (µg/ml)	32.830	8	< .001

In addition to the non-parametric test, a Dunn's Post Hoc Test was done to compare the concentrations to each other at time point 24 hours. The significant results from this test are shown in Table 8. According to the graphic representation in Figure 23, the highest significant difference belongs to the comparison between 0.635µg/ml and the rest of concentrations. Regarding the controls, five concentrations are shown to be significant excluding 0.325 and 0.635 µg/ml.

*Table 8. Dunn's Post Hoc Comparisons regarding NP µg/ml at 24 hours. Only included treatment effects against the control. Note that * p< .05, ** p < .01, *** p< .001. z= Dun's Post Hoc statistic that compares the variation between treatment groups. W_i and W_j= are the associated rank sums from each group of comparisons. P= statistical significance of the z-value.*

Comparison	z	W_i	W_j	p	
0 - 0.15	-2.069	37.583	64.042	0.039	*
0 - 2.5	-2.457	37.583	69.000	0.014	*
0 - 5.00	-2.610	37.583	70.958	0.009	**
0 - 10.00	-1.965	37.583	62.708	0.049	*
0 - 20.00	-3.099	37.583	77.208	0.002	**

5.2.4. Confocal microscopy.

To match the cell viability results obtained from the Cell Counting assay and Hoechst 3342 staining assay, confocal microscopy was utilized. The main aim being, to provide more insights regarding NPs cellular uptake and internalization and if these processes may affect cell viability.

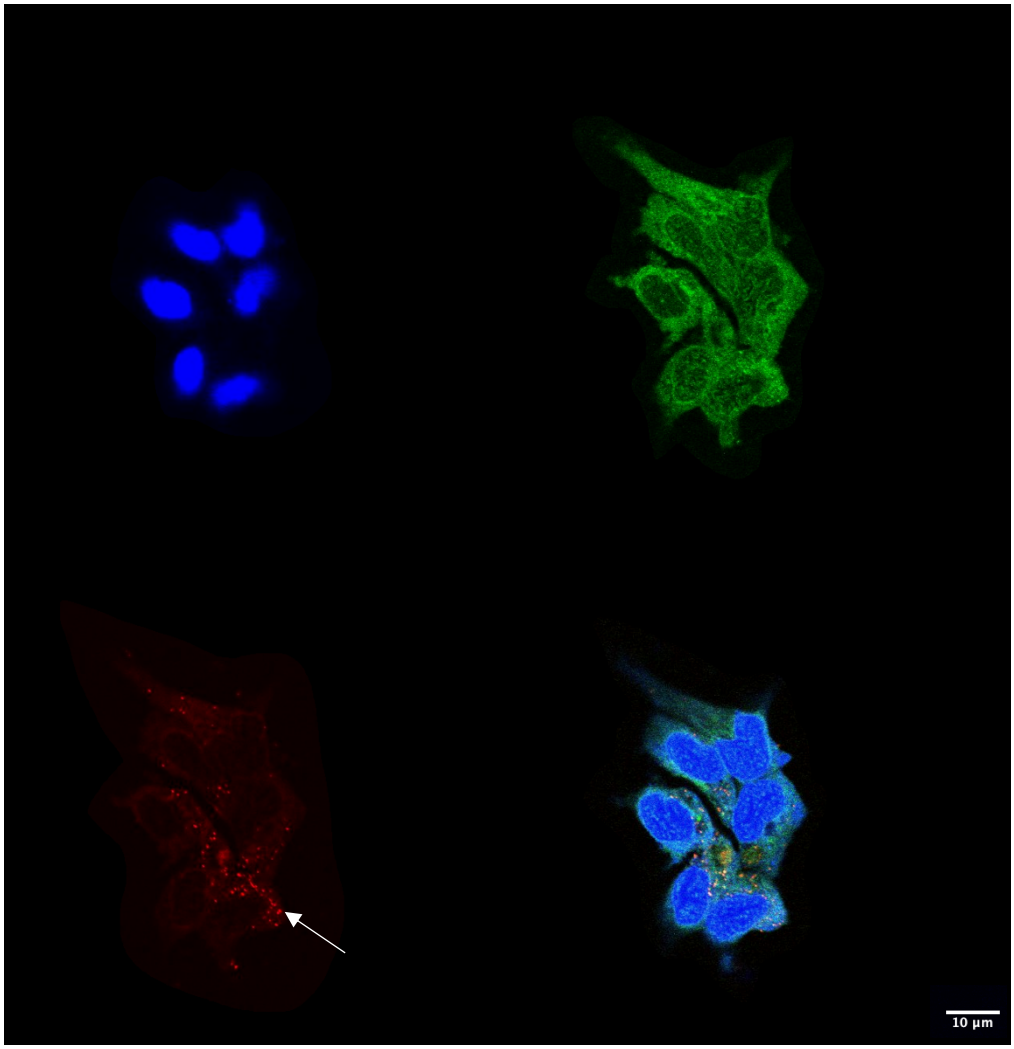

Figure 24. Localization of NPs in ZF4 cells after 48 hours of exposure to 5µg/ml fluorescent NPs. Blue: Hoechst 33342 for nuclei fluorescence. Green: Lysotracker for lysosomes. Red: Red fluorescent NPs. Arrow representing fluorescent NPs accumulated inside of the cells. Scale: 10µm.

As shown in Figure 24, cells were stained with two different dyes Hoechst 33342 for nuclei (blue) and Lysotracker for lysosomes (green) to enhanced organelle visualization. Before staining, the cells were exposed for 48 hours to 5 µg/ml red fluorescent NPs. At this time point, NPs were already internalized into the cells (see arrow). It was seen that the accumulation remained inside the cytoplasm, staying away from the nuclei, emerging through all the frames taken by the confocal microscope from the top to the bottom of the cell.

Furthermore, to narrow down the intracellular accumulation site of NPs; nuclei (Hoechst 33342, blue), lysosomes (Lysotracker, green) and mitochondria (Mytotracker, red) fluorescence was tracked.

Pictures were taken at the same time point, 48 hours, from two samples treated with the same staining method: non exposed cells (Figure 25, A.) and (Figure 25B.) exposed to non-fluorescent NPs cells. As seen in Figure 25 A., cells non exposed to NPs showed a slightly lesser red fluorescence, (mytochondria), than the cells exposed to NPs, as presented in Figure 25 B.

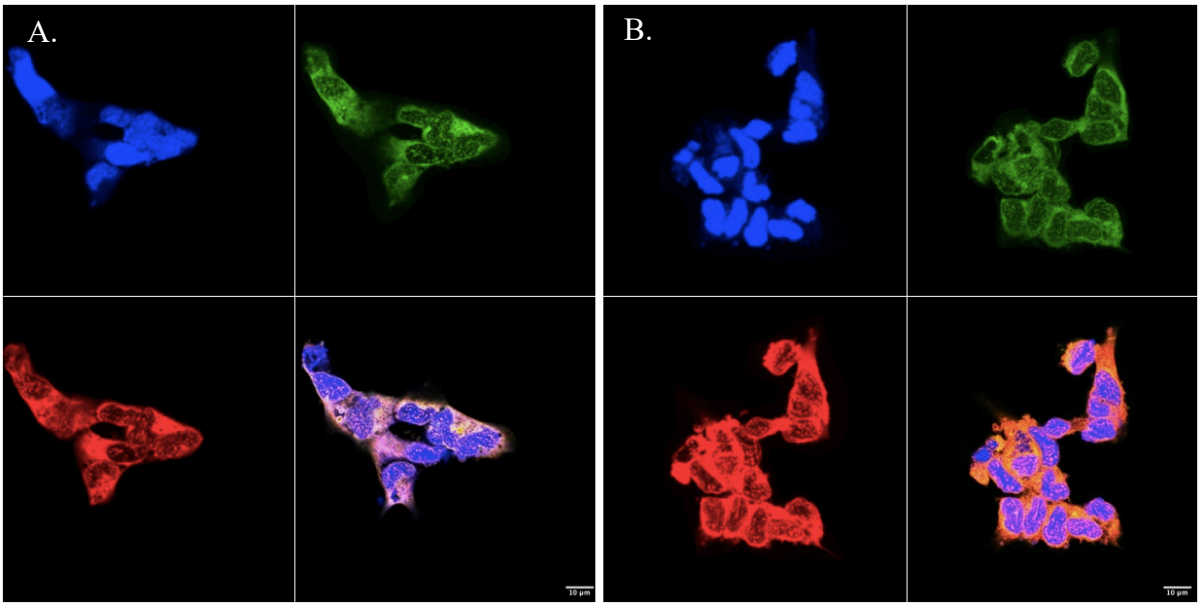

Figure 25. ZF4 cells under confocal microscopy. Sample A. represents Control ZF4 cells, dyed with Hoechst 33342 (blue for nuclei), Lysotracker (green for lysosomes) and Mytotracker (red for mitochondria). While sample B. displays ZF4 cells after 48 hours of exposure to 5µg/ml non-fluorescent NPs and dyed with Hoechst 33342 (blue for nuclei), Lysotracker (green for lysosomes) and Mytotracker (red for mitochondria). Scale: 10µm.

6. Discussion

6.1.In vivo

6.1.1. Do NPs have an effect on embryos in short term exposure?

One of the clearest outcomes from the *in vivo* study was the internalization of 100 nm PS NPs inside zebrafish embryos within 24 hours of exposure, after exposure to environmentally relevant NPs concentrations (12,5 mg/L). This has been previously documented by Pitt et al in 2018, under similar concentrations and NPs, but employing a different protocol.

Despite the fact that oral exposure has been considered one of the most significant NP uptake pathways in zebrafish, in the case of embryos, epithelial uptake is crucial, since during the whole exposure time the embryos have not developed their mouths yet (van Pomeren et al., 2017b). The olfactory pic was another location where NPs appeared accumulated inside the free-swimming early larvae. This anatomical structure has been identified as a vulnerable orifice for pathogen entrance, being filled with active immune cells (Salinas et al., 2022; Sepahi et al., 2019)

To confirm whether NPs had trespassed the chorion and had accumulated inside the embryo, two factors were considered and compared to literature: the composition of the organs targeted by NPs and the NPs size. First, the yolk sac primarily consists of fatty acids, while the olfactory pit contains neurons and epithelial cells (Miyasaka et al., 2013). It has been demonstrated that there is a strong interaction between NPs and the lipidic structure of Gram negative bacteria cell membrane, suggesting that neutral PS NPs can interact with such biomolecules (Dai et al., 2022). Regarding the olfactory pit, its NPs accumulation would be mostly defined by fact that it is an open catchment area.

Secondly, the size of NPs plays a crucial role, where smaller NPs exhibits a higher probability of entry into the zebrafish embryo (van Pomeren et al., 2017b). It is well known that the diameter of the pores in chorion measures approximately 0.5-0.7 µm, allowing enough space for 100 nm NPs to diffuse through this protective layer (Bhagat et al., 2020). As shown in the results section Figure 13, NPs are observed to be absorbed by the yolk sac after 24 hours, despite the large accumulation of NPs particles on the chorion' surface. After 96 hours, when a significant portion of the yolk sac has already been absorbed, NPs are still present inside the larvae. The yolk sac serves as their only source of nutrition during the first 96 to 122 hpf, which coincides with the larvae's full mouth development.

6.1.2. How does it affect embryo and early larvae normal development?

Following the addition of new endpoints into the FET, it was possible to broaden the investigation beyond lethality and explore additional abnormalities that may have been triggered by NPs. Following von Hellfeld et al. 2020, cases of pericardium oedema, pectoral fin and caudal tail malformations were recorded. Similar malformations were also observed in the positive control (3,4-dichloraniline), through all time points.

Among the recorded malformations, it appeared that pericardium oedema carried the highest association with lethality. Depending on how severe the pericardium oedema is, after hatching this malformation typically persists and, in most cases, leads to circulatory failure and other cardiac issues such as bradycardia (low heart rate), and kidney malformations or failure that impairs proper osmoregulation and excretory functions in the larvae (Mitchell et al., 2019; Wiegand et al., 2023). Pericardium oedema has been described to be triggered after short term exposure to chemicals (Lourenço et al., 2017) but not by 100nm NPs until now.

Regarding tail malformations (lordosis), while they do not pose an immediate threat to the larvae, they reduce their fitness. It was observed how difficult and energy-consuming was for the early larvae to move with a curved caudal fin or pectoral fins adhered to NPs. Such malformations persist throughout all developmental stages, and when reaching adulthood, it can reduce their physiological and behavioural performance, triggering several health issues including swim bladder issues and the vertebral axis compression (Boglione et al., 2013). Physical malformations after short-term NPs exposure have not been described before under the FET protocol, but it has been proved that NPs pose a neurotoxic effect on zebrafish larvae when monitoring locomotor activity (Chen et al. 2017).

6.1.3. Do NPs have a lethal effect on embryos?

The next question to answer was whether NPs possess a toxic or lethal impact on zebrafish embryos and early larvae. Despite conducting the Fish Embryo Acute Toxicity Test (FET) more than five times using different sets of NPs concentrations, the LC_{50} could not be determined under this particular experimental procedure. Similar studies have shared the same concern, for instance, no embryotoxic effects at concentrations up to 100 mg/L of polyethylene microplastics (PE MPs) could be observed within 96 hours (Cormier et al. 2019) . Likely, the FET protocol may not be suitable enough to evaluate the toxicity of NPs towards zebrafish embryos (Cormier et al., 2019; Stelzer et al., 2018). However, the FET can be easily improved by incorporating additional endpoints, such as the assessment of malformations or other types of alterations (von Hellfeld et al., 2020).

Moreover, out of the four indicators proposed by the FET, only two were observed as valuable. The first indicator was embryo coagulation, typically observed at 24 hours post-fertilization (hpf) or later, when usually a partial coagulation is exhibited in some parts of the embryo. The second parameter that proved to be useful was the absence of heartbeat, which can only be recorded from 48 hpf onwards. This parameter was particularly helpful when examining the positive control, as the embryos were fully developed, yet their heart rates began to decrease or cease at 96 hpf. The tail bud attachment was only informative on one occasion; while the lack of somite formation was never observed, not even regarding the positive control.

6.1.4. Does NP trigger an increased inflammatory response?

As already mentioned, following amputation or injury of a tissue, the inflammatory response is activated, and a method to track it is following neutrophil mobilization. As seen in the results, both the control cut and exposed cuts (1 mg/L and 10 mg/L) showed the activation and mobilization of neutrophils, which migrated to the injured area to repair the wound and cause inflammation. Our hypothesis stated that, upon exposure to NPs, there would be an increased mobilization of neutrophils to the injured and newly regenerated area, as they would instinctively respond to any potential threats, such as, attempting to breach or enter the fish body. Across all timepoints (Figure 16), the neutrophil count at 10 mg/L showed a statistically significant increase compared to 1mg/L and control cut (0 mg/L). But, at 96 hours, both treatments, showed a comparable statistically significant difference in neutrophil mobilization against the control no cut. Additionally, the neutrophil count for control cut (0 mg/L) at 96 hours had reached almost the same number as the control no cut, indicating a lack of statistical difference between them. After these results, our initial hypothesis could be accepted, meaning that neutrophils do not abandon the previously amputated area after being fully regenerated.

It is important to note that this protocol is highly dependent on two factors: (a) the efficiency of amputation practice, achieving reliable cuts in the same location on each larva is challenging and requires skills and experience; (b) the immune system of the larvae; large variations in neutrophil numbers have been observed among all samples, indicating significant differences in individual larval development.

6.1.5. Does it affect normal larval processes like regeneration?

As mentioned before, due to the limited experience with this technique, achieving precise and consistent cuts was particularly challenging. As a result, getting accurate and reliable results was very difficult.

In the context of the current study, statistical significance in regeneration rate was not observed between the treatment groups (cut 1 mg/L and cut 10 mg/L) to the control cut (0 mg/L). Even though, the non-parametric test, Kruskal-Wallis, showed a p-value that accepted our hypothesis, we can conclude that NPs do not inhibit regeneration rate but it does have an effect.

Since this is the first time the inflammation process after NPs exposure has been studied in young zebrafish larvae using this technique, limited information is available for comparison or analysis.

6.1.6. Future perspectives: *in vivo*.

Regarding the FET, it would be suitable to focus mostly on sublethal effects and to conduct observations to monitor viability and malformations over several weeks, especially, after the complete reabsorption of the yolk sac. It would be interesting to assess if previously exposed larvae and adults, still exhibit fluorescence coming from NPs in any other tissue. Comparing this with normal development and fish fitness would provide insights into the potential impacts of NP in the long term.

To obtain more accurate results, it would be recommended to repeat the amputation procedure. I t was shown that after 96 hours, a large number of neutrophils remained in the newly regenerated area. It would be interested to keep track of neutrophils number during a chronic exposure, to determine when does the inflammatory response finally resolves. This time, the emphasis should be on studying macrophages, since it would be interesting to attempt to track them to see if their behaviour gets impacted by NPs. The challenges met with macrophages were primarily related to the interference caused by the red fluorescence expressed by NPs and by xanthophores coming from Mpeg mutants (Gray et al., 2011). Perhaps, using different mutant strains for macrophages or other colours for fluorescent NPs could simplify the process.

It would also be interesting to conduct more extensive and precise research into the current and future concentrations of NPs in the environment, especially in freshwater ecosystems. One of the challenges encountered during this research was the lack of reliable literature regarding environmentally relevant concentrations of NPs in this ecosystem. Some of the few studies available providing this kind of information are mostly focused on marine ecosystems or can be considered outdated (Al-Sid-Cheikh et al., 2018). The need of having recent information is because the NPs concentration in aquatic ecosystems can fluctuate a lot within a short time period, due to the unstable degradation rate of mega-, meso- and microplastics giving rise to NPs and the continuous and unregulated plastic waste input into the environment (da Costa et

al., 2016; Jambeck et al., 2015; Redondo-Hasselerharm et al., 2020; Thushari & Senevirathna, 2020).

Moreover, it is essential to consider that, from the beginning of plastic production in 1960 until the year 2015, a shocking amount of over 5,000 million metric tons of plastic waste has been recorded to be generated and uncontrollably discarded. This alarming trend suggests that by the year 2050, it is expected to exceed 25,000 million metric tons of plastic waste in all its various forms and sizes (Geyer et al., 2017)

For these several reasons, estimating an accurately predicted NPs concentration in the environment is proved to be a terrifying task. Conducting a thorough and accurate assessment of NPs' environmental concentrations would contribute significantly to the understanding of the potential impacts they may have on the health of both nature and biodiversity health and help inform future research and risk assessment efforts.

6.2. In vitro

6.2.1. Does short-term exposure to NPs have an effect on ZF4 cells? What is the effect? Is there a dose-response effect?

As indicated in the Results section (Figure 18), the start of the cell counting experiment exhibited unfavourable outcomes. The seeding success rate decreased by 65%, with the lowest results attributed to the use of ZF4 cells with the highest passage number (P23). A very high passage number affects the viability of the cells, being more susceptible to cell death than the ones present in the first passages. Therefore, the results obtained under these conditions may have varied slightly from the ones expected from the protocol.

A slightly distinct trend of a dose-response effect was observed, although numerous outliers were present through all time points and concentrations, with the biggest variations occurring at 72 hours. These variations can be attributed to factors such as pipetting and manipulation errors, as well as the cell seeding success due to changes in confluency from a T75 flask to the 24 well plates that own a well area of 1.86 cm^2.

Image analysis granted three significant observations. Firstly, an alteration in cell shape as the concentration of nanoparticles (NPs) increased (Figure 19-Figure 22). The cells transitioned from a slender morphology with typical cytoplasmic projections to a more round-like appearance. This change was observed as early as 24 hours and persisted at 48, 72, and 96 hours, when the cell morphology looked slightly different.

At the last time point, two distinct types of dead cells were observed. The control and concentrations up to 2.5 µg/ml exhibited some rounded and condensed morphology (white under phase contrast microscopy), suggesting that the cytoplasmic content had accumulated inside the cells (Figure 22). This phenomenon was also observed in the control, which could indicate cell death due to the high confluency achieved in the well and the absence of fresh medium throughout 96 hours. On the contrary, a notable contrast in cell morphology was observed between the cells treated with NPs concentrations ranging from 5 to 20 µg/ml. In this case, the cells appeared as perfect bubbles with an empty interior (translucent under phase contrast microscopy), adhered to the remains of the cytoskeleton. These cells did not exhibit characteristics of apoptotic cells, yet they cannot be definitively classified as necrotic cells based only on imaging. These two kinds of dead cells have not been previously described on ZF4 cultures after NPs exposure.

To reinforce the findings obtained from the cell counting assay, a Hoechst 33342 test was conducted. However, the results were inconclusive. The only instance where a trend of inhibition was observed was at 24 hours. At the same time, from 24 to 72 hours, the trends suggest the presence of a biphasic inhibition effect of NPs. This implies that lower concentrations triggered an inhibitory effect on cell viability, followed by a period without inhibition or even positive impacts until the central concentration was reached, after which the inhibitory effect re-started again (Liu et al., 2007). This biphasic inhibition trend hasn't been found so far in the current literature regarding NPs, ZF4 cells and cytotoxicity.

The dissimilarities between the imaging results and cell viability data, resulted in a new question: do NPs penetrate the cells, and if so, how do they interact with cellular organelles such as mitochondria and lysosomes?

2.1.NP inside the cells and its interaction with cell organelles.

There is a substantial lack of literature regarding neutral PS NPs internalization within eukaryotic cells. The presence of other molecules or compounds attached to NPs determines NPs uptake and its subsequent distribution within the cell (Quevedo et al., 2021; Yang & Wang, 2022). It has been proved that NPs coated or attached to molecules, such as amino or carboxyl groups, enhance the chances of NPs internalization by interacting with the cell membranes. This interaction is mostly due to the surface charge of the amino and carboxyl groups, owning positive and negative charges, respectively. Not in eukaryotic cells, but in bacteria, the positively charged NH_2-PSNPs showed a higher efficiency in lipidic membrane translocation

while negatively charged COOH-PSNPs exhibited a minimal or significantly reduced translocation (Dai et al., 2022)

In this study, following a 48-hour exposure period, confocal microscopy was utilized to capture images to identify fluorescent nanoparticles (f-NPs) within the ZF4 cells. A relatively low concentration of 5μg/ml was employed to ensure cell viability was not compromised. The imaging results thereby confirmed the internalization of 100nm NPs inside the cells.

Additionally, an attempt to assess the relationship between NPs and mitochondrial activity under confocal microscopy was made. Even though the results obtained only by confocal microscopy are not consistent enough, a higher mitochondrial fluorescence intensity coming from exposed cells could be appreciated when compared to the mitochondrial fluorescence coming from the control. This enhanced fluorescent intensity could be related to a higher mitochondrial activity. Mitochondrial dysfunction after 100 nm NPs has already been observed by the assessment of intracellular reactive oxygen species (ROS) production (Yang and Wang 2022).

2.2.Optimizing the cell line.

Due to the lack of information and experience regarding ZF4 cells, generating a considerable quantity of cells within a limited timeframe presented significant challenges. This initial setback delayed the possibility of conducting a large and trustworthy number of experiments. By the time sufficient experience was gained, the cells had already passed through multiple passages, leading to earlier cell death and lower seeding success.

The initial ZF4 culture (Passage 1) included a total of 2 million cells, but, during the initial weeks, the cells started to decrease rapidly in number after each subcultivation process. During the first 2-3 passages, throughout trypsinization -the moment 0.025% Trypsin is added, the cells were incubated at 37ºC, ensuring Trypsin activity. Trypsin is mainly used to de-attach the cell culture from the surface of the flask. When an unexpected reduction of cell growth was noticed, the incubation at 37ºC immediately stopped. Thus, ZF4 cells proved to be very sensitive to heat shock. Subsequently, there was a notable increase in cell number, but still, the cell doubling time was very slow.

The second change made in the subcultivation protocol, involved a modified medium, incorporating 20% heat-inactivated fetal bovine serum (FBS) into DMEM/F12. The objective of inactivating the FBS was to neutralize any potential inhibitors of cell growth present in the serum (Johnson, 2012).

It is well-known that every cell type possesses a distinct cellular density, which plays a critical role in cell functionality and viability (Neurohr & Amon, 2020). In this case, it was needed to increase the cell number seeded in a T75 flask (total of 75 cm2) from 6,600 cells per cm2 (our initial guess based on the subcultivation of Caco2 cells), to 26,600 cells/cm2 for ZF4 cells, in order to achieve the same cellular density (80% confluency), after a 48-hour period. This was a trial-error discovery due to the little literature regarding the ZF4 cell line culture.

2.1.Future perspectives, *in vitro*.

Regarding the non-defined dead cells observed under phase contrast microscopy, an apoptosis assay utilizing flow cytometry could be employed to obtain more accurate results. It would be interesting to define and describe these kinds of cells for future investigations with ZF4 cells.

As for the internalization of f-NPs inside ZF4 cells, the exact entry pathway remains unknown Further investigations to understand this NPs uptake into the cells could be very remarkable, mostly to study the role of the cell membrane considering this new kind of macromolecule. Nevertheless, the uptake of NPs through the cellular membrane has been proven to induce severe damage to the cell membrane (Yang & Wang, 2022).

Although the observations obtained provided the previously mentioned indications, it would be valuable to apply specific assays such as MTT for mitochondrial metabolic activity, flow cytometry for mitochondrial membrane permeability and dysregulation detection, flow cytometry or assay kits for ROS production detection; to further elucidate and quantify the effects of NPs on mitochondrial function.

3. *In vivo vs. in vitro*.

After completing all the protocols and analysing the obtained results, a final comparison between both studies was done. This comparison could be done because during the experimental design, some requisites for both *in vivo* and *in vitro* studies were implemented. First, to keep the same model organism for both studies; the possibility of using Caco-2 cells was considered because it was not necessary to produce a cell culture and due to all protocols being already optimized. The second concern was to follow all experiments for the same exposure time, an acute exposure. And most important, keeping everything under the same scope: NPs potential toxicity and its internalization on zebrafish.

One of the main advantages of having completed these two studies is that they provided complementary insights. While the *in vivo* part offered the big picture of the issue, *in vitro* allowed a closer look. As an example, while lethal effects could not be observed *in vivo*, *in*

vitro, a statistically significant cell lethality was found. The importance of having these two studies under the same aim gives to one what the other one was lacking.

As a second advantage, after performing both experiments together, the validation and correlation of results are easier. For instance, when *in vivo* results for NPs internalization (Figure 13) were obtained, it was thought that part of the fluorescence showed could be due to the leaching of the fluorochrome from the NPs. However, after checking NPs internalization into the cell (Figure 24), a more precise and defined outcome was acquired. In this case, there was a correlation between the size of the fluorescent spot with the known size of the NPs used; while *in vivo* only a large area of strong fluorescence emission was shown.

In summary, conducting both studies at the same time under the same aim has facilitated a better understanding of the results obtained by both parties and then, to relate them to each other.

7. Conclusion.

Nanoplastics (NPs) short-term exposure on zebrafish was found to have an effect on both *in vivo* and *in vitro* studies. In the *in vivo* studies, the FET (OECD no.263) indicated that acute exposure to 200 mg/L NPs for 96 hours increased the likelihood of zebrafish embryos developing malformations such as pericardium oedema by 15%. Additionally, NPs were found to penetrate the chorion when exposed to environmentally relevant concentrations, subsequently accumulating in both yolk sac and olfactory pit persisting within the embryo after hatching.

Continuing with the *in vivo* studies, after caudal fin amputation, it could be concluded that exposure to NPs environmentally relevant concentrations did not inhibit the larval capacity of regeneration. Furthermore, only in larvae exposed to NPs concentrations, neutrophils appear to remain in the newly regenerated area as if the inflammatory response hasn't finished yet.

As for the *in vitro* results, both NPs concentrations and time are directly proportional to cell number decrease, meaning that increasing concentrations of NPs decrease cell viability of ZF4 cells with increasing time. Moreover, after 48 of exposure, NPs show to be transported inside the cell membrane and accumulated within the cytoplasm.

For future investigations, it would be beneficial to further explore the outcomes that could not be fully addressed within this investigation.

8. References

Abdolahpur Monikh, F., Grundschober, N., Romeijn, S., Arenas-Lago, D., Vijver, M. G., Jiskoot, W., & Peijnenburg, W. J. G. M. (2019). Development of methods for extraction and analytical characterization of carbon-based nanomaterials (nanoplastics and carbon nanotubes) in biological and environmental matrices by asymmetrical flow field-flow fractionation. *Environmental Pollution*, *255*. https://doi.org/10.1016/j.envpol.2019.113304

Aleström, P., D'Angelo, L., Midtlyng, P. J., Schorderet, D. F., Schulte-Merker, S., Sohm, F., & Warner, S. (2020). Zebrafish: Housing and husbandry recommendations. *Laboratory Animals*, *54*(3), 213–224. https://doi.org/10.1177/0023677219869037

Al-Sid-Cheikh, M., Rowland, S. J., Stevenson, K., Rouleau, C., Henry, T. B., & Thompson, R. C. (2018). Uptake, Whole-Body Distribution, and Depuration of Nanoplastics by the Scallop Pecten maximus at Environmentally Realistic Concentrations. *Environmental Science and Technology*, *52*(24), 14480–14486. https://doi.org/10.1021/acs.est.8b05266

Amaral-Zettler, L. A., Zettler, E. R., Slikas, B., Boyd, G. D., Melvin, D. W., Morrall, C. E., Proskurowski, G., & Mincer, T. J. (2015). The biogeography of the Plastisphere: Implications for policy. *Frontiers in Ecology and the Environment*, *13*(10), 541–546. https://doi.org/10.1890/150017

Andrady, A. L. (2011). Microplastics in the marine environment. *Marine Pollution Bulletin*, *62*(8), 1596–1605. https://doi.org/https://doi.org/10.1016/j.marpolbul.2011.05.030

Azevedo-Santos, V. M., Brito, M. F. G., Manoel, P. S., Perroca, J. F., Rodrigues-Filho, J. L., Paschoal, L. R. P., Gonçalves, G. R. L., Wolf, M. R., Blettler, M. C. M., Andrade, M. C., Nobile, A. B., Lima, F. P., Ruocco, A. M. C., Silva, C. V., Perbiche-Neves, G., Portinho, J. L., Giarrizzo, T., Arcifa, M. S., & Pelicice, F. M. (2021). Plastic pollution: A focus on freshwater biodiversity. In *Ambio* (Vol. 50, Issue 7, pp. 1313–1324). Springer Science and Business Media B.V. https://doi.org/10.1007/s13280-020-01496-5

Baharvand, H., Ashtiani, S. K., Valojerdi, M. R., Shahverdi, A., Taee, A., & Sabour, D. (2004). Establishment and in vitro differentiation of a new embryonic stem cell line from human blastocyst. *Differentiation*, *72*(5), 224–229. https://doi.org/10.1111/J.1432-0436.2004.07205005.X

Baig, A., Zubair, M., Zafar, M. N., Farid, M., Nazar, M. F., & Sumrra, S. H. (2022). 11 - Nanobiodegradation of plastic waste. In H. M. N. Iqbal, M. Bilal, T. A. Nguyen, & G. Yasin (Eds.), *Biodegradation and Biodeterioration At the Nanoscale* (pp. 239–259). Elsevier. https://doi.org/https://doi.org/10.1016/B978-0-12-823970-4.00011-7

Bakare, A. B., Daniel, J., Stabach, J., Rojas, A., Bell, A., Henry, B., & Iyer, S. (2021). Quantifying mitochondrial dynamics in patient fibroblasts with multiple developmental defects and mitochondrial disorders. *International Journal of Molecular Sciences*, *22*(12). https://doi.org/10.3390/ijms22126263

Ballent, A., Corcoran, P. L., Madden, O., Helm, P. A., & Longstaffe, F. J. (2016). Sources and sinks of microplastics in Canadian Lake Ontario nearshore, tributary and beach sediments. *Marine Pollution Bulletin*, *110*(1), 383–395. https://doi.org/10.1016/j.marpolbul.2016.06.037

Barros, L. F., Kanaseki, T., Sabirov, R., Morishima, S., Castro, J., Bittner, C. X., Maeno, E., Ando-Akatsuka, Y., & Okada, Y. (2003). Apoptotic and necrotic blebs in epethelial cells display similar neck diameters but different kinase dependency. *Cell Death and Differentiation*, *10*(6), 687–697. https://doi.org/10.1038/sj.cdd.4401236

Barua, S., & Mitragotri, S. (2014). Challenges associated with penetration of nanoparticles across cell and tissue barriers: A review of current status and future prospects. In *Nano Today* (Vol. 9, Issue 2, pp. 223–243). Elsevier B.V. https://doi.org/10.1016/j.nantod.2014.04.008

Behzadi, S., Serpooshan, V., Tao, W., Hamaly, M. A., Alkawareek, M. Y., Dreaden, E. C., Brown, D., Alkilany, A. M., Farokhzad, O. C., & Mahmoudi, M. (2017). Cellular uptake of nanoparticles: Journey inside the cell. In *Chemical Society Reviews* (Vol. 46, Issue 14, pp. 4218–4244). Royal Society of Chemistry. https://doi.org/10.1039/c6cs00636a

Bhagat, J., Zang, L., Nishimura, N., & Shimada, Y. (2020). Zebrafish: An emerging model to study microplastic and nanoplastic toxicity. In *Science of the Total Environment* (Vol. 728). Elsevier B.V. https://doi.org/10.1016/j.scitotenv.2020.138707

Boglione, C., Gisbert, E., Gavaia, P., E. Witten, P., Moren, M., Fontagné, S., & Koumoundouros, G. (2013). Skeletal anomalies in reared European fish larvae and juveniles. Part 2: main typologies, occurrences and causative factors. *Reviews in Aquaculture*, *5*(s1), S121–S167. https://doi.org/https://doi.org/10.1111/raq.12016

Bundschuh, M., Filser, J., Lüderwald, S., McKee, M. S., Metreveli, G., Schaumann, G. E., Schulz, R., & Wagner, S. (2018). Nanoparticles in the environment: where do we come from, where do we go to? In *Environmental Sciences Europe* (Vol. 30, Issue 1). Springer Verlag. https://doi.org/10.1186/s12302-018-0132-6

Busch, M., Brouwer, H., Aalderink, G., Bredeck, G., Kämpfer, A. A. M., Schins, R. P. F., & Bouwmeester, H. (2023). Investigating nanoplastics toxicity using advanced stem cell-based intestinal and lung in vitro models. *Frontiers in Toxicology*, *5*. https://doi.org/10.3389/ftox.2023.1112212

Canedo, A., & Rocha, T. L. (2021). Zebrafish (Danio rerio) using as model for genotoxicity and DNA repair assessments: Historical review, current status and trends. *Science of The Total Environment*, *762*, 144084. https://doi.org/10.1016/J.SCITOTENV.2020.144084

Canesi, L., Balbi, T., Fabbri, R., Salis, A., Damonte, G., Volland, M., & Blasco, J. (2017). Biomolecular coronas in invertebrate species: Implications in the environmental impact of nanoparticles. In *NanoImpact* (Vol. 8, pp. 89–98). Elsevier B.V. https://doi.org/10.1016/j.impact.2017.08.001

Chen, Q., Gundlach, M., Yang, S., Jiang, J., Velki, M., Yin, D., & Hollert, H. (2017). Quantitative investigation of the mechanisms of microplastics and nanoplastics toward zebrafish larvae locomotor activity. *Science of the Total Environment*, *584–585*, 1022–1031. https://doi.org/10.1016/j.scitotenv.2017.01.156

Choi, T. Y., Choi, T. I., Lee, Y. R., Choe, S. K., & Kim, C. H. (2021). Zebrafish as an animal model for biomedical research. In *Experimental and Molecular Medicine* (Vol. 53, Issue 3, pp. 310–317). Springer Nature. https://doi.org/10.1038/s12276-021-00571-5

Cole, M., Lindeque, P., Halsband, C., & Galloway, T. S. (2011). Microplastics as contaminants in the marine environment: A review. In *Marine Pollution Bulletin* (Vol. 62, Issue 12, pp. 2588–2597). https://doi.org/10.1016/j.marpolbul.2011.09.025

Cormier, B., Batel, A., Cachot, J., Bégout, M. L., Braunbeck, T., Cousin, X., & Keiter, S. H. (2019). Multi-Laboratory Hazard Assessment of Contaminated Microplastic Particles by Means of Enhanced Fish Embryo Test With the Zebrafish (Danio rerio). *Frontiers in Environmental Science*, *7*. https://doi.org/10.3389/fenvs.2019.00135

da Costa Araújo, A. P., de Melo, N. F. S., de Oliveira Junior, A. G., Rodrigues, F. P., Fernandes, T., de Andrade Vieira, J. E., Rocha, T. L., & Malafaia, G. (2020). How much are microplastics harmful to the health of amphibians? A study with pristine polyethylene microplastics and Physalaemus cuvieri. *Journal of Hazardous Materials*, *382*, 121066. https://doi.org/10.1016/J.JHAZMAT.2019.121066

da Costa, J. P., Santos, P. S. M., Duarte, A. C., & Rocha-Santos, T. (2016). (Nano)plastics in the environment - Sources, fates and effects. In *Science of the Total Environment* (Vols 566–567, pp. 15–26). Elsevier B.V. https://doi.org/10.1016/j.scitotenv.2016.05.041

Dai, S., Ye, R., Huang, J., Wang, B., Xie, Z., Ou, X., Yu, N., Huang, C., Hua, Y., Zhou, R., & Tian, B. (2022). Distinct lipid membrane interaction and uptake of differentially charged nanoplastics in bacteria. *Journal of Nanobiotechnology*, *20*(1). https://doi.org/10.1186/s12951-022-01321-z

Dick, M. K., Miao, J. H., & Limaiem, F. (2023). *Histology, Fibroblast*.

Domenech, J., de Britto, M., Velázquez, A., Pastor, S., Hernández, A., Marcos, R., & Cortés, C. (2021). Long-term effects of polystyrene nanoplastics in human intestinal Caco-2 cells. *Biomolecules*, *11*(10). https://doi.org/10.3390/biom11101442

Driever, W., & Rangini, Z. (1993). CHARACTERIZATION OF A CELL LINE DERIVED FROM ZEBRAFISH (BRACHYDANIO RERIO) EMBRYOS. In *In Vitro Cell. Dev. Biol* (Vol. 29).

Elmore, S. (n.d.). *Apoptosis: A Review of Programmed Cell Death*.

Fischer, E. K., Paglialonga, L., Czech, E., & Tamminga, M. (2016). Microplastic pollution in lakes and lake shoreline sediments – A case study on Lake Bolsena and Lake Chiusi (central Italy). *Environmental Pollution*, *213*, 648–657. https://doi.org/10.1016/J.ENVPOL.2016.03.012

Gallo, F., Fossi, C., Weber, R., Santillo, D., Sousa, J., Ingram, I., Nadal, A., & Romano, D. (2018). Marine litter plastics and microplastics and their toxic chemicals components: the need for urgent preventive measures. In *Environmental Sciences Europe* (Vol. 30, Issue 1). Springer Verlag. https://doi.org/10.1186/s12302-018-0139-z

Galluzzi, L., Vitale, I., Aaronson, S. A., Abrams, J. M., Adam, D., Agostinis, P., Alnemri, E. S., Altucci, L., Amelio, I., Andrews, D. W., Annicchiarico-Petruzzelli, M., Antonov, A. V., Arama, E., Baehrecke, E. H., Barlev, N. A., Bazan, N. G., Bernassola, F., Bertrand, M. J. M., Bianchi, K., … Kroemer, G. (2018). Molecular mechanisms of cell death: Recommendations of the Nomenclature Committee on Cell Death 2018. In *Cell Death and Differentiation* (Vol. 25, Issue 3, pp. 486–541). Nature Publishing Group. https://doi.org/10.1038/s41418-017-0012-4

Geyer, R., Jambeck, J. R., & Law, K. L. (2017). Production, use, and fate of all plastics ever made. *Science Advances*, *3*(7), e1700782. https://doi.org/10.1126/sciadv.1700782

Gonçalves, M., Schmid, K., Andrade, M. C., Andrades, R., Pegado, T., & Giarrizzo, T. (2020). Are the tidal flooded forests sinks for litter in the Amazonian estuary? *Marine Pollution Bulletin*, *161*, 111732. https://doi.org/10.1016/J.MARPOLBUL.2020.111732

Gray, C., Loynes, C. A., Whyte, M. K. B., Crossman, D. C., Renshaw, S. A., & Chico, T. J. A. (2011). Simultaneous intravital imaging of macrophage and neutrophil behaviour during inflammation using a novel transgenic zebrafish. *Thrombosis and Haemostasis*, *105*(5), 811–819. https://doi.org/10.1160/TH10-08-0525

Gregory, M. R. (2009). Environmental implications of plastic debris in marine settings-entanglement, ingestion, smothering, hangers-on, hitch-hiking and alien invasions. In *Philosophical Transactions of the Royal Society B: Biological Sciences* (Vol. 364, Issue 1526, pp. 2013–2025). Royal Society. https://doi.org/10.1098/rstb.2008.0265

Harvie, E. A., & Huttenlocher, A. (2015). Neutrophils in host defense: new insights from zebrafish. *Journal of Leukocyte Biology*, *98*(4), 523–537. https://doi.org/10.1189/jlb.4mr1114-524r

Iucn, ©. (n.d.). *IUCN website IUCN issues briefs: Twitter: @IUCN www.iucn.org www.iucn.org/issues-briefs*. www.iucn.org/issues-briefs

Jambeck, J. R., Geyer, R., Wilcox, C., Siegler, T. R., Perryman, M., Andrady, A., Narayan, R., & Law, K. L. (2015). Plastic waste inputs from land into the ocean. *Science*, *347*(6223), 768–771. https://doi.org/10.1126/science.1260352

Johnson, M. (2012). Fetal Bovine Serum. *Materials and Methods*, *2*. https://doi.org/10.13070/MM.EN.2.117

Kanwal, H., Nadeem, H., Azeem, F., Rasul, I., Muzammil, S., Zubair, M., Imran, M., Afzal, M., & Siddique, M. H. (2023). Chapter 5 - Generation and impact of microplastics and nanoplastics from bioplastic sources. In A. Sarkar, B. Sharma, & S. Shekhar (Eds.), *Biodegradability of Conventional Plastics* (pp. 83–99). Elsevier. https://doi.org/https://doi.org/10.1016/B978-0-323-89858-4.00003-8

Kelpsiene, E., Torstensson, O., Ekvall, M. T., Hansson, L. A., & Cedervall, T. (2020). Long-term exposure to nanoplastics reduces life-time in Daphnia magna. *Scientific Reports*, *10*(1). https://doi.org/10.1038/s41598-020-63028-1

Kwon, B. G., Amamiya, K., Sato, H., Chung, S. Y., Kodera, Y., Kim, S. K., Lee, E. J., & Saido, K. (2017). Monitoring of styrene oligomers as indicators of polystyrene plastic pollution in the North-West Pacific Ocean. *Chemosphere*, *180*, 500–505. https://doi.org/10.1016/J.CHEMOSPHERE.2017.04.060

Kwon, B. G., Koizumi, K., Chung, S.-Y., Kodera, Y., Kim, J.-O., & Saido, K. (2015). Global styrene oligomers monitoring as new chemical contamination from polystyrene plastic marine pollution. *Journal of Hazardous Materials*, *300*, 359–367. https://doi.org/https://doi.org/10.1016/j.jhazmat.2015.07.039

Leonelli, S., & Ankeny, R. A. (2013). What makes a model organism? *Endeavour*, *37*(4), 209–212. https://doi.org/https://doi.org/10.1016/j.endeavour.2013.06.001

Liu, Y. B., Guo, J. Z., & Chiappinelli, V. A. (2007). Nicotinic receptor-mediated biphasic effect on neuronal excitability in chick lateral spiriform neurons. *Neuroscience*, *148*(4), 1004–1014. https://doi.org/10.1016/j.neuroscience.2007.07.009

Lourenço, J., Marques, S., Carvalho, F. P., Oliveira, J., Malta, M., Santos, M., Gonçalves, F., Pereira, R., & Mendo, S. (2017). Uranium mining wastes: The use of the Fish Embryo Acute Toxicity Test (FET) test to evaluate toxicity and risk of environmental discharge. *Science of the Total Environment*, *605–606*, 391–404. https://doi.org/10.1016/j.scitotenv.2017.06.125

Manshian, B. B., Pokhrel, S., Mädler, L., & Soenen, S. J. (2018). The impact of nanoparticle-driven lysosomal alkalinization on cellular functionality. *Journal of Nanobiotechnology*, *16*(1). https://doi.org/10.1186/s12951-018-0413-7

Marana, M. H., Poulsen, R., Thormar, E. A., Clausen, C. G., Thit, A., Mathiessen, H., Jaafar, R., Korbut, R., Hansen, A. M. B., Hansen, M., Limborg, M. T., Syberg, K., & von Gersdorff Jørgensen, L. (2022). Plastic nanoparticles cause mild inflammation, disrupt metabolic pathways, change the gut microbiota and affect reproduction in zebrafish: A full generation multi-omics study. *Journal of Hazardous Materials*, *424*. https://doi.org/10.1016/j.jhazmat.2021.127705

Mariano, S., Tacconi, S., Fidaleo, M., Rossi, M., & Dini, L. (2021). Micro and Nanoplastics Identification: Classic Methods and Innovative Detection Techniques. *Frontiers in Toxicology*, *3*. https://doi.org/10.3389/ftox.2021.636640

Meyers, J. R. (2018). Zebrafish: Development of a Vertebrate Model Organism. *Current Protocols in Essential Laboratory Techniques*, *16*(1). https://doi.org/10.1002/cpet.19

Mindell, J. A. (2012). Lysosomal Acidification Mechanisms. *Annual Review of Physiology*, *74*(1), 69–86. https://doi.org/10.1146/annurev-physiol-012110-142317

Mitchell, C. A., Reddam, A., Dasgupta, S., Zhang, S., Stapleton, H. M., & Volz, D. C. (2019). Diphenyl Phosphate-Induced Toxicity during Embryonic Development. *Environmental Science and Technology*, *53*(7), 3908–3916. https://doi.org/10.1021/acs.est.8b07238

Miyasaka, N., Wanner, A. A., Li, J., Mack-Bucher, J., Genoud, C., Yoshihara, Y., & Friedrich, R. W. (2013). Functional development of the olfactory system in zebrafish. *Mechanisms of Development*, *130*(6), 336–346. https://doi.org/https://doi.org/10.1016/j.mod.2012.09.001

Neurohr, G. E., & Amon, A. (2020). Relevance and Regulation of Cell Density. In *Trends in Cell Biology* (Vol. 30, Issue 3, pp. 213–225). Elsevier Ltd. https://doi.org/10.1016/j.tcb.2019.12.006

Ng, E. L., Huerta Lwanga, E., Eldridge, S. M., Johnston, P., Hu, H. W., Geissen, V., & Chen, D. (2018). An overview of microplastic and nanoplastic pollution in agroecosystems. In *Science of the Total Environment* (Vol. 627, pp. 1377–1388). Elsevier B.V. https://doi.org/10.1016/j.scitotenv.2018.01.341

Nguyen, L. H., Nguyen, B. S., Le, D. T., Alomara, T. S., AlMasoud, N., Ghotekar, S., Oza, R., Raizada, P., Singh, P., & Nguyen, V. H. (2023). A concept for the biotechnological minimizing of emerging plastics, micro- and nano-plastics pollutants from the environment: A review. *Environmental Research*, *216*. https://doi.org/10.1016/j.envres.2022.114342

Nguyen-Chi, M., Laplace-Builhé, B., Travnickova, J., Luz-Crawford, P., Tejedor, G., Lutfalla, G., Kissa, K., Jorgensen, C., & Djouad, F. (2017). TNF signaling and macrophages govern fin regeneration in zebrafish larvae. *Cell Death and Disease*, *8*(8). https://doi.org/10.1038/CDDIS.2017.374

Norton, W., & Bally-Cuif, L. (2010). *Adult zebrafish as a model organism for behavioural genetics*. http://www.biomedcentral.com/1471-2202/11/90

Pereira, S., Malard, V., Ravanat, J. L., Davin, A. H., Armengaud, J., Foray, N., & Adam-Guillermin, C. (2014). Low doses of gamma-irradiation induce an early bystander effect

in zebrafish cells which is sufficient to radioprotect cells. *PLoS ONE*, *9*(3). https://doi.org/10.1371/journal.pone.0092974

Pitt, J. A., Kozal, J. S., Jayasundara, N., Massarsky, A., Trevisan, R., Geitner, N., Wiesner, M., Levin, E. D., & Di Giulio, R. T. (2018). Uptake, tissue distribution, and toxicity of polystyrene nanoparticles in developing zebrafish (Danio rerio). *Aquatic Toxicology*, *194*, 185–194. https://doi.org/10.1016/j.aquatox.2017.11.017

Quevedo, A. C., Lynch, I., & Valsami-Jones, E. (2021). Mechanisms of silver nanoparticle uptake by embryonic zebrafish cells. *Nanomaterials*, *11*(10). https://doi.org/10.3390/nano11102699

Rada, B. (2019). Neutrophil extracellular traps. In *Methods in Molecular Biology* (Vol. 1982, pp. 517–528). Humana Press Inc. https://doi.org/10.1007/978-1-4939-9424-3_31

Rasool, F. N., Saavedra, M. A., Pamba, S., Perold, V., Mmochi, A. J., Maalim, M., Simonsen, L., Buur, L., Pedersen, R. H., Syberg, K., & Jelsbak, L. (2021). Isolation and characterization of human pathogenic multidrug resistant bacteria associated with plastic litter collected in Zanzibar. *Journal of Hazardous Materials*, *405*. https://doi.org/10.1016/j.jhazmat.2020.124591

Redondo-Hasselerharm, P. E., Gort, G., Peeters, E. T. H. M., & Koelmans, A. A. (2020). Nano- and microplastics affect the composition of freshwater benthic communities in the long term. *Science Advances*, *6*(5), eaay4054. https://doi.org/10.1126/sciadv.aay4054

Renshaw, S. A., Loynes, C. A., Trushell, D. M. I., Elworthy, S., Ingham, P. W., & Whyte, M. K. B. (2006). *A transgenic zebrafish model of neutrophilic inflammation*. https://doi.org/10.1182/blood-2006

Salinas, I., Garcia, B., & Casadei, E. (2022). Discovery of an organized nasopharynx-associated lymphoid tissue in the nasal cavity of rainbow trout and its role in secondary adaptive immune responses to nasal vaccines. *J Immunol 1*, *1_Supplement*(124.19), 208.

Scholz, S., Fischer, S., Gündel, U., Küster, E., Luckenbach, T., & Voelker, D. (2008). The zebrafish embryo model in environmental risk assessment - Applications beyond acute toxicity testing. In *Environmental Science and Pollution Research* (Vol. 15, Issue 5, pp. 394–404). https://doi.org/10.1007/s11356-008-0018-z

Sendra, M., Pereiro, P., Yeste, M. P., Mercado, L., Figueras, A., & Novoa, B. (2021a). Size matters: Zebrafish (Danio rerio) as a model to study toxicity of nanoplastics from cells to the whole organism. *Environmental Pollution*, *268*. https://doi.org/10.1016/j.envpol.2020.115769

Sendra, M., Pereiro, P., Yeste, M. P., Mercado, L., Figueras, A., & Novoa, B. (2021b). Size matters: Zebrafish (Danio rerio) as a model to study toxicity of nanoplastics from cells to the whole organism. *Environmental Pollution*, *268*. https://doi.org/10.1016/j.envpol.2020.115769

Sepahi, A., Kraus, A., Casadei, E., Johnston, C. A., Galindo-Villegas, J., Kelly, C., García-Moreno, D., Muñoz, P., Mulero, V., Huertas, M., & Salinas, I. (2019). Olfactory sensory neurons mediate ultrarapid antiviral immune responses in a TrkA-dependent manner. *Proceedings of the National Academy of Sciences of the United States of America*, *116*(25), 12428–12436. https://doi.org/10.1073/pnas.1900083116

Silva, A. B., & Marmontel, M. (2009). *INGESTÃO DE LIXO PLÁSTICO COMO PROVÁVEL CAUSA MORTIS DE PEIXE-BOI AMAZÔNICO (Trichechus Inunguis NATTERER, 1883)* (Issue 1).

Silva Brito, R., Canedo, A., Farias, D., & Rocha, T. L. (2022). Transgenic zebrafish (Danio rerio) as an emerging model system in ecotoxicology and toxicology: Historical review, recent advances, and trends. In *Science of the Total Environment* (Vol. 848). Elsevier B.V. https://doi.org/10.1016/j.scitotenv.2022.157665

Stelzer, J. A. A., Rosin, C. K., Bauer, L. H., Hartmann, M., Pulgati, F. H., & Arenzon, A. (2018). Is fish embryo test (FET) according to OECD 236 sensible enough for delivering quality data for effluent risk assessment? *Environmental Toxicology and Chemistry*, *37*(11), 2925–2932. https://doi.org/10.1002/etc.4215

Organisation for Economic Co-operation and Development (OECD)). (2013). *Test No. 236: Fish Embryo Acute Toxicity (FET) Test*. https://doi.org/10.1787/9789264203709-EN

The Ocean Cleanup. (2023). *Rivers*. https://theoceancleanup.com/rivers/

Thushari, G. G. N., & Senevirathna, J. D. M. (2020). Plastic pollution in the marine environment. In *Heliyon* (Vol. 6, Issue 8). Elsevier Ltd. https://doi.org/10.1016/j.heliyon.2020.e04709

Uemoto, T., Abe, G., & Tamura, K. (2020). Regrowth of zebrafish caudal fin regeneration is determined by the amputated length. *Scientific Reports*, *10*(1). https://doi.org/10.1038/s41598-020-57533-6

van Pomeren, M., Brun, N. R., Peijnenburg, W. J. G. M., & Vijver, M. G. (2017a). Exploring uptake and biodistribution of polystyrene (nano)particles in zebrafish embryos at different developmental stages. *Aquatic Toxicology*, *190*, 40–45. https://doi.org/10.1016/j.aquatox.2017.06.017

van Pomeren, M., Brun, N. R., Peijnenburg, W. J. G. M., & Vijver, M. G. (2017b). Exploring uptake and biodistribution of polystyrene (nano)particles in zebrafish embryos at different developmental stages. *Aquatic Toxicology*, *190*, 40–45. https://doi.org/10.1016/j.aquatox.2017.06.017

von Hellfeld, R., Brotzmann, K., Baumann, L., Strecker, R., & Braunbeck, T. (2020). Adverse effects in the fish embryo acute toxicity (FET) test: a catalogue of unspecific morphological changes versus more specific effects in zebrafish (Danio rerio) embryos. *Environmental Sciences Europe*, *32*(1). https://doi.org/10.1186/s12302-020-00398-3

Wayman, C., & Niemann, H. (2021). The fate of plastic in the ocean environment-a minireview. In *Environmental Science: Processes and Impacts* (Vol. 23, Issue 2, pp. 198–212). Royal Society of Chemistry. https://doi.org/10.1039/d0em00446d

Wiegand, J., Avila-Barnard, S., Nemarugommula, C., Lyons, D., Zhang, S., Stapleton, H. M., & Volz, D. C. (2023). Triphenyl phosphate-induced pericardial edema in zebrafish embryos is dependent on the ionic strength of exposure media. *Environment International*, *172*. https://doi.org/10.1016/j.envint.2023.107757

Yang, M., & Wang, W. X. (2022). Differential cascading cellular and subcellular toxicity induced by two sizes of nanoplastics. *Science of the Total Environment*, *829*. https://doi.org/10.1016/j.scitotenv.2022.154593

9. Table of Figures.

Figure 1. Plastic waste degradation in the environment. Plastic waste is released into the environment and once it gets into aquatic systems plastic degradation starts. Once in the water, plastic undergoes a fragmentation process after being exposed to UV radiation which weakens the bonds between plastic monomers, enabling other kinds of degradation such as microbial degradation and mechanical fragmentation due to wave movements. This fragmentation results in smaller plastic particles, MPs and NPs, and the consequent release of all the additives chemically attached during plastic production. (Abdolahpur Monikh et al., 2019). 10

Figure 2. Plastic waste production and mismanagement around the world. It is represented how out of the total plastic production, there's a portion of plastic waste that is being mismanaged, meaning that is directly released to the environment without being recycled or re-used. (Jambeck et al., 2015) 13

Figure 3. Morphology of a normal zebrafish embryo at 24hpf and larvae at 96hpf. Arrows indicate each structure (von Hellfeld et al., 2020). 16

Figure 4. FET endpoints at 24h (1, 2, 3, 4, 5) and 96h (6, 7, 8). Arrows and asterisks as indicators. (1) 1.5hpf embryo at the time the exposure starts (cleavage period: 8 cells). (2) Coagulated embryo. (3) Normal somite formation (4) Lack of somite formation. (5) Non-detachment of tail bud. (6) Pericardium oedema (fluid accumulation in the heart). (7) Scoliosis (malformation). (8) Lordosis (malformation). OECD protocol and (von Hellfeld et al., 2020) 17

Figure 5. Mechanism of cell death after NH2-PS proposed by Meng Yang et al (2022). ZF4 cells are exposed to NPs of two sizes 100nm and 1000nm. After passing the cell membrane, NPs are deposited in lysosomes, increasing the volume of the acidic compartments (altering lysosomal alkalinization and acidification), triggering lysosomal permeabilization resulting in the release of ROS and Cathepsin B/L and D into the cytoplasm. The discharge of these molecules causes mitochondria damage and cascading effects such as caspase 3/7 activation, which provokes loss of the mitochondria cell integrity and eventually cell death. (Yang & Wang, 2022) 22

Figure 6. Breeding procedure description. (1) Sorting of females and males adults from the desired genotypes. (2) Keep in dark conditions until the start of the light cycle for the breeding process. (3) After 1 hour of mating, the eggs are fertilized and ready to be collected, counted, and sorted. Made with biorrender.com. 25

Figure 7. Subcultivation process protocol description. (1) Remove the old medium. (2) Rinse with 10 ml of Trypsin 0.25% without EDTA and remove. Add 2ml of 0.25% Trypsin without EDTA and incubate for 5 minutes at room temperature. (4) Add 8 ml of medium and resuspend breaking cell aggregations. Transfer to a 15ml Falcon Tube. (5) Use 200µl to test cell number in Coulter Counter. (6) Add $2x10^6$ cells to a new T75 flask with 10ml of new medium at room temperature. Return the flask to the incubator. Made with biorrender.com. 26

Figure 8. Fish Embryo Acute Toxicity Test protocol visualization. (1) Eggs collection and sorting 1.5 hours post fertilization following the mentioned criteria. (2) Seeding of chosen eggs in 24 wells-plates. Each plate counted with four wells as internal controls with just sterile facility water. (3) Imaging analysis every 24h to record the test parameters. Made with biorrender.com. 28

Figure 9. Fin amputation scheme. (1) Anaesthetize and fin tail cut in 4 days post-fertilization larvae. (2) Transfer of larvae to Petri dishes for recovery and Nanoplastics exposure. (3) Imaging and analysis every 24 hours. Made with biorrender.com. 30

Figure 10. Cell counting assay description. (1) Subcultivation and cell number estimation. Cell seeding in 24-well plates. (2) after 24 hours, images of each well are taken. Cell exposure to NPs starts. (3) Remove the old medium. Wash the wells with 0,1 ml of PBS without Ca, and Mg and add 0,2 ml of 0.25% Trypsin without EDTA. (4) Incubate at 37º and 5% CO_2 for 20 minutes. (5) Add 0,8 ml of PBS without Ca, Mg and resuspend making enough pressure to the bottom of the wells to de-attach as many cells as possible. (6) Cell counting with Coulter Counter in 10ml of saline solution. Made with biorrender.com. 31

Figure 11. Hoechst staining protocol visualization. (1) Subcultivation and cell number estimation. Seeding in 96 well-plates. (2) After 24 hours, start cell exposure. (3) Remove the old medium and add 100 µl per well of Hoechst 33342 (5 µg/ml) in room temperature DMEM and incubate at 28ºC and 5% CO_2 for 90 minutes. (4) 90 minutes after, remove the old medium and rinse once with PBS with Ca, Mg. Add 100 µl of PBS with Ca, Mg. (6) Read fluorescence in a microplate reader. Made with biorrender.com. 32

Figure 12. Visualization of the cell staining carried out for the second confocal microscopy experiment. Cells were seeded and exposed to (a) 5µg/ml fluorescent-NPS; and (b) 5µg/ml non-fluorescent-NPs on poly-D-lysine coated glass dishes. In both cases keeping a control without exposure to NPs. 48 hours after exposure, the cells were stained as represented above (a) with Hoechst 33342 and LysoTracker Green; and (b) with Hoechst 33342, LysoTracker

Green and MitoTracker Orange. After waiting for the stipulated time and finishing the staining protocol, pictures were taken with the confocal microscope. Made by biorrender.com 34

Figure 13. Zebrafish wild-type embryos after 24 hours of exposure to red fluorescent NPs. Pictures were taken under fluorescence microscopy. From A. to E. embryos exposed to increasing concentrations of NPs (mentioned above). Figure A, a.1. represents NPs accumulation inside the yolk sac extension, while a.2. points at eh NPs accumulation in the yolk sac. Figure E, e.1 indicates NPs aggregates on the surface of the chorion. Scale: 200µm. 36

Figure 14. Zebrafish wild-type embryos and larvae under fluorescent microscopy. A. Zebrafish embryo with tail bud malformation at 24 hours after exposure to the positive control (3,4-dichloraniline). B. Zebrafish early larvae at 72 hours after exposure to the positive control (3,4-dichloraniline); b.1. indicating lordosis malformation; and b.2. implying pericardium oedema. C. Zebrafish early larvae in the moment of hatching, 72 hours after exposure to the positive control (3,4-dichloraniline); c.1. indicating pericardium oedema. D. Zebrafish early larvae 72 hours after exposure to 200 mg/L red fluorescent NPs (f-NPs); d.1. indicating f-NPs inside the olfactory pit; and d.2. indicating f-NPs accumulation inside the yolk sac and d.3. yolk sac extension. Scale: 200µm. 37

Figure 15. Regeneration rate in obtain-types (WT) and a double transgenic line with fluorescent neutrophils and macrophages (DbTg) zebrafish after caudal fin amputation. The mean of the regeneration rate in µm (±SD, n:18), is represented in the Y axis, plotted against every time point (24, 48, 72 and 96 hours), on the X axis. At the same time, the data is grouped by controls (control no cut and control cut 0 mg/l) and treatments (cut 1 mg/l and cut 10 mg/l). P-values represented the significance of the comparisons made with Duns Post Toc Test between each treatment against de control no cut. Note that: * $p < .05$, ** $p < .01$, *** $p < .001$. 38

Figure 16. Bar plot of neutrophils number in regenerated area of Double Transgenic (DbTg) zebrafish after caudal fin amputation. The dependent variable, the number of neutrophils (±SD, n:6), is represented in the Y axis, plotted against every time point (24, 48, 72 and 96 hours), in the X axis while being grouped by controls (control and control cut 0 mg/L) and treatments (cut 1 mg/L and cut 10 mg/L). P-values represented the significance of the comparisons made with Duns Post Toc Test between each treatment against de control no cut. Note that: * $p < .05$, ** $p < .01$, *** $p < .001$ 40

Figure 17. Caudal fin amputation and regeneration through the different time points. Neutrophils are represented in green. Macrophages, xanthophores and NPs in red. Note in Control 24 hours it is indicated where the cut was performed. The cut was made through the whole tail fin, being careful to not touch the body of the zebrafish larvae. Scale: 200µm. 41

Figure 18. Effect of NPs on ZF4 cell number. The dependent variable, mean of the cell number of 3 replicates (±SD, n:12), is represented on the Y axis, plotted against every time point (24, 48, 72 and 96 hours); on the X axis, while remaining grouped by increasing NP concentrations. Each time point represents a different 24-well plate, meaning that for "48 hours" the 24-well plate was not disturbed until the exposure time was reached. Each colour represents the different NP concentrations, cells were exposed to. P-values represented the significance of the comparisons made with Duns Post Toc Test between each NP concentration against de control. Note that: * p < .05, ** p < .01, *** p < .001..... 44

Figure 19. ZF4 cells after 24 hours of NPs exposure. Each picture, from A to F, corresponds to the cells exposed to each NPs concentration (from 0 to 20 µg/ml). Scale: 200 µm..... 44

Figure 20. ZF4 cells after 48 hours of NPs exposure. Each picture, from A to F, corresponds to the cells exposed to each NPs concentration (from 0 to 20 µg/ml). Scale: 200 µm..... 45

Figure 21. ZF4 cells after 72 hours of NPs exposure. Each picture, from A to F, corresponds to the cells exposed to each NPs concentration (from 0 to 20 µg/ml). Scale: 200 µm..... 45

Figure 22. ZF4 cells after 96 hours of NPs exposure. Each picture, from A to F, corresponds to the cells exposed to each NPs concentration (from 0 to 20 µg/ml). Scale: 200 µm..... 46

Figure 23. Inhibition % of NP on ZF4 cells under increasing concentrations: 0.15, 0.315, 0.625, 1.25, 2.5, 5, 10, 20 µg/ml NP (shown on top of error lines). Note that the concentrations are plotted on their log10 form. Control (0µg/ml) is not represented but it equals 0% inhibition. Each line joins together the different points which represents the mean of the NP inhibition % (± SD, n=24) on cells exposed to the previously mentioned concentrations. The four sets 24, 48, 72 and 96 hours represents the exposure time. 48

Figure 24. Localization of NPs in ZF4 cells after 48 hours of exposure to 5µg/ml fluorescent NPs. Blue: Hoechst 33342 for nuclei fluorescence. Green: Lysotracker for lysosomes. Red: Red fluorescent NPs. Arrow representing fluorescent NPs accumulated inside of the cells. Scale: 10µm. 49

Figure 25. ZF4 cells under confocal microscopy. Sample A. represents Control ZF4 cells, dyed with Hoechst 33342 (blue for nuclei), Lysotracker (green for lysosomes) and Mytotracker (red for mitochondria). While sample B. displays ZF4 cells after 48 hours of exposure to 5µg/ml non-fluorescent NPs and dyed with Hoechst 33342 (blue for nuclei), Lysotracker (green for lysosomes) and Mytotracker (red for mitochondria). Scale: 10µm..... 50